

Review of Selected Features of the Natural System Model, and Suggestions for Applications in South Florida

Water Resources Investigations Report 97-4039



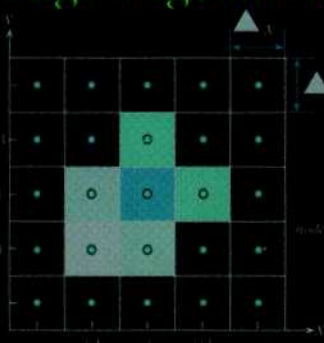
U.S. GEOLOGICAL SURVEY

Prepared in cooperation with the

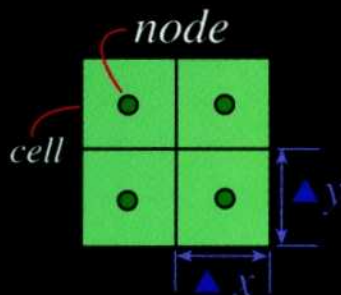
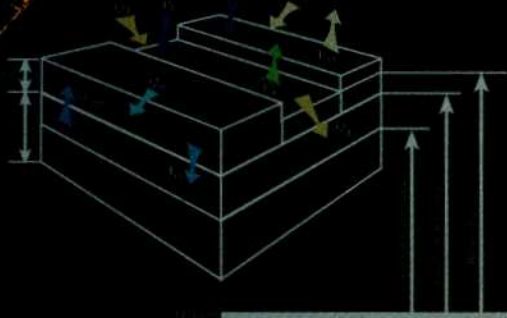
U.S. Army Corps of Engineers, Jacksonville District

Pre-drainage vegetation and topography

Climatic data



$$h_{i,j,t+1}$$



NSM

Natural System Model

Regional scale model

South Florida

[Click here to return to USGS publications](#)

Review of Selected Features of the Natural System Model, and Suggestions for Applications in South Florida

By JERAD D. BALES, JANICE M. FULFORD, and ERIC SWAIN

U.S. GEOLOGICAL SURVEY

Water-Resources Investigations Report 97-4039

Prepared in cooperation with the

U.S. Army Corps of Engineers, Jacksonville District

Raleigh, North Carolina
1997



U.S. DEPARTMENT OF THE INTERIOR
BRUCE BABBITT, Secretary

U.S. GEOLOGICAL SURVEY
Gordon P. Eaton, Director



The use of firm, trade, and brand names in this report is for identification purposes only and does not constitute endorsement by the U.S. Geological Survey.

For additional information write to:

District Chief
U.S. Geological Survey
227 N. Bronough Street, Suite 3015
Tallahassee, FL 32301

Copies of this report can be purchased from:

U.S. Geological Survey
Branch of Information Services
Box 25286, Federal Center
Denver, CO 80225

CONTENTS

Abstract.....	1
Introduction	2
Purpose and scope	6
Previous investigations	7
Acknowledgments	10
Governing equations and boundary conditions	10
River-system flow equations.....	11
Overland flow	14
Equations	14
Boundary conditions.....	20
Ground-water flow.....	20
Equations	20
Boundary conditions.....	22
Review of selected features of the Natural System Model.....	23
Initial and boundary conditions	24
Computational grid size and time step	24
River system	28
Overland-flow system	32
Natural System Model version 4.3 and two-dimensional hydrodynamic model overland-flow simulations.....	33
Natural System Model version 4.4	34
Conclusions	34
Suggestions for application of the Natural System Model	36
Suggested modifications	36
Appropriate applications.....	37
Issues for possible future investigation.....	39
References	39
Appendix—List of variables.....	41

FIGURES

1.–3. Maps showing:	
1. Generalized south Florida land use and hydrology during the early 1900's and the mid-1990's	3
2. Selected management areas of the south Florida watershed	4
3. The Natural System Model grid for south Florida and inset showing relation between nodes and cells	5
4.–8. Diagrams showing:	
4. Variables used in the river-system equation. (A) Longitudinal view along the length of a river system, and (B) Side view of a cell within a river segment.....	13
5. Intracell and intercell hydrologic processes represented within the Natural System Model	14
6. Overland and ground-water flow variables in the Natural System Model	15
7. Computational modules or active cells in a grid fragment for solution of overland flow between cells for calculations for $H_{i,j,t+1}$ proceeding from (A) west to east and north to south, and (B) east to west and south to north	16
8. Computational modules or active cells in a grid fragment for the ground-water computations for $h_{i,j,t+1}$ proceeding from (A) west to east and south to north, and (B) east to west and north to south.....	22
9.–13. Graphs showing:	
9. Combined effects of computational cell size and time step on mean ponding depth and mean depth to ground water for a grid velocity of 0.12 foot per second.....	26

10. Combined effects of computational cell size and time step on mean ponding depth and mean depth to ground water for a grid velocity of about 0.35 foot per second.....	27
11. Stages computed for eight NSM rivers by using the original NSM river outflow algorithm and a modified algorithm based on the Manning equation.....	30
12. Jupiter River stage computed by using the original NSM river-system algorithm and a modified river-system algorithm in which there is no coupling between the river and ground-water systems	31
13. Stages computed for four NSM river systems by using the original NSM river-system algorithm and a modified algorithm in which there is no coupling between the overland-flow and river systems	31

TABLES

1. Review issues and approaches for review	7
2. Mean ponding depths and depths to ground water as a function of computational grid size and time step.....	25
3. Simulated water-level differences, ponding depths, and depths to ground water made by using NSM version 4.3 (2-mile grid, 6-hour time step) and other combinations of grid size and time step for October 1965 conditions	28
4. Summary of tests of river-system algorithms	29
5. Comparison of NSM and TRIM results.....	33

CONVERSION FACTORS, VERTICAL DATUM, AND ACRONYMS

Multiply	By	To obtain
Length		
inch (in.)	2.54	centimeter
foot (ft)	0.3048	meter
mile (mi)	1.609	kilometer
Area		
acre	0.4047	hectare
square mile (mi ²)	2.590	square kilometer
Flow		
foot per second (ft/s)	0.3048	meter per second
cubic foot per second (ft ³ /s)	0.02832	cubic meter per second

Sea level: In this report “sea level” refers to the National Geodetic Vertical Datum of 1929 (NGVD of 1929)—A geodetic datum derived from a general adjustment of the first-order level nets of both the United States and Canada, formerly called Sea Level Datum of 1929.

Acronyms:

EAA	Everglades Agricultural Area
ENP	Everglades National Park
LEC	Lower East Coast
NSM	Natural System Model
RMS	root mean square
SFWMD	South Florida Water Management District
SFWMM	South Florida Water Management Model
TRIM	tidal residual, intertidal mudflat
USGS	U.S. Geological Survey
WCA	Water Conservation Area

Review of Selected Features of the Natural System Model, and Suggestions for Applications in South Florida

By Jerad D. Bales, Janice M. Fulford, and Eric Swain

ABSTRACT

A study was conducted to review selected features of the Natural System Model, version 4.3. The Natural System Model is a regional-scale model that uses recent climatic data and estimates of historic vegetation and topography to simulate pre-canal-drainage hydrologic response in south Florida. Equations used to represent the hydrologic system and the numerical solution of these equations in the model were documented and reviewed. Convergence testing was performed using 1965 input data, and selected other aspects of the model were evaluated.

Some conclusions from the evaluation of the Natural System Model include the following observations. Simulations were generally insensitive to the temporal resolution used in the model. However, reduction of the computational cell size from 2-mile by 2-mile to 2/3-mile by 2/3-mile resulted in a decrease in spatial mean ponding depths for October of 0.35 foot for a 3-hour time step.

Review of the computer code indicated that there is no limit on the amount of water that can be transferred from the river system to the overland-flow system, on the amount of seepage from the river to the ground-water system, on evaporation from the river system, or on evapotranspiration from the overland-flow system. Oscillations of 0.2 foot or less in simulated river stage were identified and attributed to a volume limiting function which is applied in solution of the overland-flow equations. The computation of the resistance

coefficient is not consistent with the computation of overland-flow velocity. Ground-water boundary conditions do not always ensure a no-flow condition at the boundary. These inconsistencies had varying degrees of effects on model simulations, and it is likely that simulations longer than 1 year are needed to fully identify effects. However, inconsistencies in model formulations should not be ignored, even if the effects of such errors on model results appear to be small or have not been clearly defined.

The Natural System Model can be a very useful tool for estimating pre-drainage hydrologic response in south Florida. The model includes all of the important physical processes needed to simulate a water balance. With a few exceptions, these hydrologic processes are represented in a reasonable manner using empirical, semi-empirical, and mechanistic relations. The data sets that have been assembled to represent physical features, and hydrologic and meteorological conditions are quite extensive in their scope.

Some suggestions for model application were made. Simulation results from the Natural System Model need to be interpreted on a regional basis, rather than cell by cell. The available evidence suggests that simulated water levels should be interpreted with about a plus or minus 1 foot uncertainty. It is probably not appropriate to use the Natural System Model to estimate pre-drainage discharges (as opposed to hydroperiods and water levels) at a particular location or across a set of adjacent computational cells. All simulated results for computational cells within about 10 miles of the

model boundaries have a higher degree of uncertainty than results for the interior of the model domain. It is most appropriate to interpret the Natural System Model simulation results in connection with other available information. Stronger linkages between hydrologic inputs to the Everglades and the ecological response of the system would enhance restoration efforts.

INTRODUCTION

The south Florida ecosystem has been greatly altered during the last 100 years (fig. 1). Drainage of the south Florida watershed began in the early 1880's, and by the early 1990's about 50 percent of the historic Everglades had been drained by ditches and canals. In response to flooding and to provide water for a variety of human uses, a complex water-management system that includes levees, well fields, pumps, canals, and control structures was constructed throughout south Florida. This system provides a steady supply of freshwater to a growing population of more than 4 million people in the Lower East Coast (LEC) Water Supply Plan service areas; to agricultural areas primarily in the Everglades agricultural area (EAA) and east of the Everglades National Park (ENP); to the Big Cypress National Preserve; and to the ENP and subsequently Florida Bay (fig. 2).

The South Florida Water Management Model (SFWMM) was developed by the South Florida Water Management District (SFWMD) in the late 1970's and early 1980's to simulate the hydrology of this water-management system in south Florida (MacVicar and others, 1984). The SFWMM is a regional model that includes simulation of hydrologic processes (evapotranspiration, surface flow, infiltration, ground-water flow, canal flow, and canal-aquifer interactions) and water-management activities (canal stage maintenance, water-control structure operation, and water withdrawals) in an approximately 7,600-square-mile (mi²) area. The effects of water-management scenarios on time-varying ground- and surface-water conditions and on canal flows are simulated for selected static land uses and management schemes. Time-varying historic rainfall and evapotranspiration data from 1965 to 1990, actual or predicted ground-water withdrawals, and irrigation demands for the LEC areas are used as model inputs for the simulations. The model is calibrated using time-series ground- and

surface-water-level data collected from more than 100 monitoring stations in the modeled area.

The Natural System Model (NSM) simulates the hydrologic response of pre-canal-drainage south Florida by using 1965–90 climatic data and estimated physical features of the modeled region. The NSM was developed directly from the SFWMM by the SFWMD in about 1989 and was established as version 3.4 (Perkins and MacVicar, 1991). Following a review (Fennema, 1992), modifications were made by the SFWMD and version 3.6 was established, and limited documentation was published (Fennema and others, 1994). The NSM has been undergoing more or less continuous updates since that time, and changes have been documented primarily in SFWMD memoranda and internal reports.

The NSM uses the same climatic input data and model parameters, and similar model algorithms and computational schemes as the SFWMM. However, to simulate the hydrologic response of the natural system, SFWMM physical features, such as topography, vegetation, land use, and hydromodifications, have been adjusted to represent pre-drainage conditions. The vegetation coverage for the NSM was derived from a landscape map of south Florida for the early 1900's, and pre-drainage channels or rivers were identified from surveys completed between 1855 and 1870. The NSM topography is generally the same as that used in the SFWMM, except in areas of known soil subsidence.

Overland flow is the dominant water-transport mechanism in the natural system, whereas ground-water and canal flows dominate in the managed, or existing system. Significant overland flows do occur in the natural areas, such as the ENP, of the SFWMM domain. In addition to overland flow, processes included in the NSM are rainfall, evapotranspiration, infiltration, ground-water flow, and flows in some small, coastal rivers (fig. 3). Inflows to Lake Okeechobee include estimated "natural" river inflows, overland flow, ground-water flow, and rainfall. Outflows from the lake to south Florida occur when the lake stage exceeds the estimated land-surface elevation of the southern rim of the lake.

The NSM domain covers an area of about 9,312 mi² (fig. 3) and consists of 2,328 computational cells, 2-mile (mi) by 2-mi each. Water level, velocity, land elevation, vegetation, and land use are assumed to be uniform within each cell, and flow may enter or exit the cell along any of the four sides. Rather than modeling

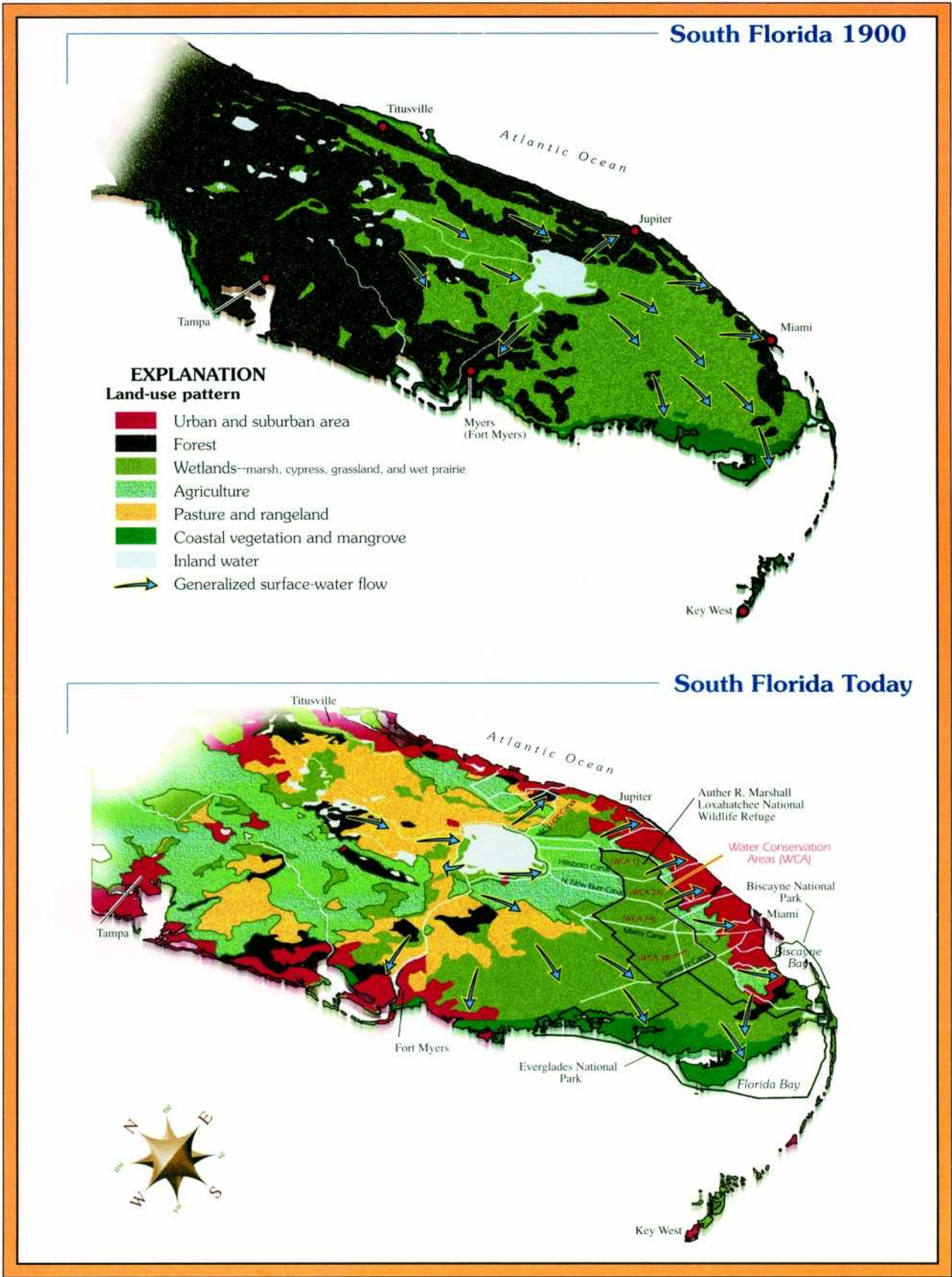


Figure 1. Generalized south Florida land use and hydrology during the early 1900's and the mid-1990's.

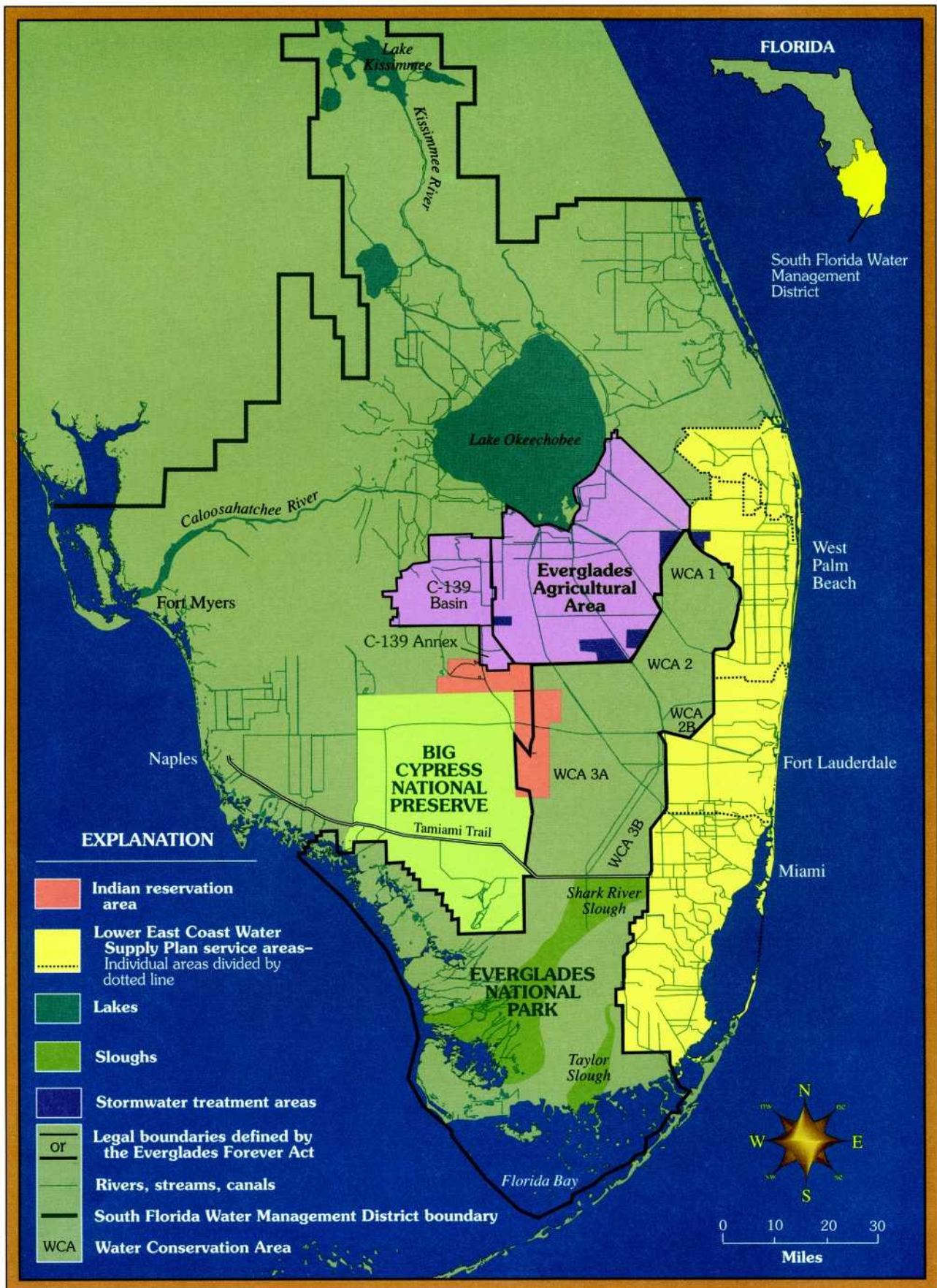


Figure 2. Selected management areas of the south Florida watershed.

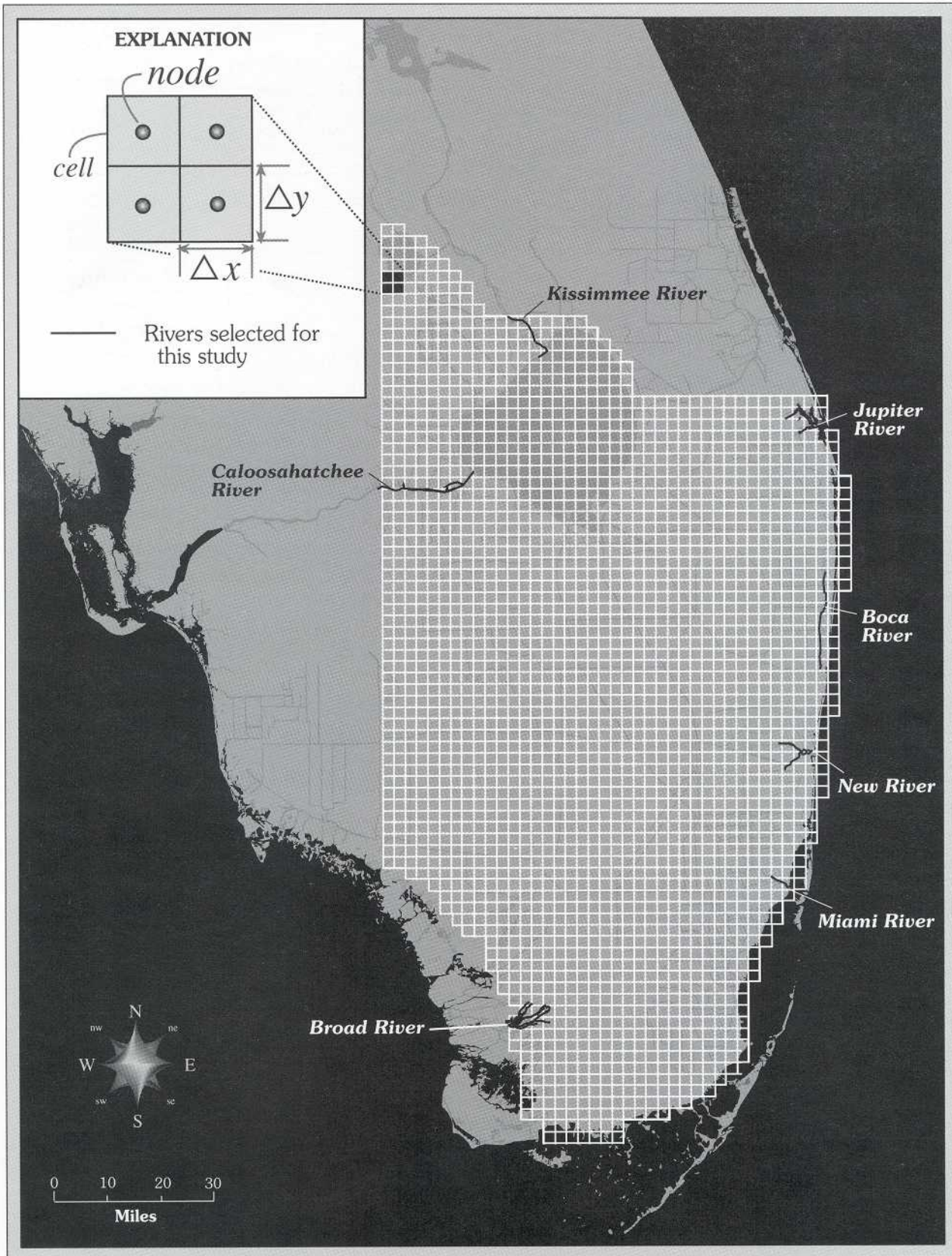


Figure 3. The Natural System Model grid for south Florida and inset showing relation between nodes and cells.

all physical processes explicitly (such as the complete three-dimensional turbulent flow, and the heat and water transport associated with evapotranspiration), the NSM includes several parameters which are used to simplify descriptions of these complex processes.

The NSM is somewhat unique in that the model is fundamentally linked to the SFWMM. Model parameters for the NSM are obtained from the calibrated SFWMM, because the NSM cannot be calibrated directly. This means that if the SFWMM is modified and subsequently recalibrated, then model parameters in the NSM also must be changed and new NSM simulations made. Moreover, algorithms describing hydrologic processes in the two models must be the same in order for model parameters in the NSM to have the same meaning in the NSM as in the calibrated SFWMM. Consequently, it is generally true that changes in either the NSM or the SFWMM must be accompanied by changes in the other model, followed by a new calibration of the SFWMM.

The accuracy and validity of the NSM cannot be tested using traditional modeling approaches because hydrologic data from the pre-drainage south Florida ecosystem do not exist for comparison with model results. Moreover, accurate, detailed information on historic vegetative and topographic conditions required for the NSM simulations is largely unavailable, leading to additional uncertainty in model output. Calibrated model parameters from the SFWMM are transferred directly to the NSM, but these parameters may represent different processes in the two models for some parts of the model domain, particularly where there have been changes in land use, topography, vegetation, and drainage patterns.

In the past, the performance of the NSM was evaluated by using three approaches. First, because the fundamental algorithms used in the NSM are the same as those used in the SFWMM, and because the SFWMM appears to perform adequately, it was assumed that the NSM properly simulates the important hydrologic processes. Second, a series of tests was performed by the SFWMD to identify (1) the sensitivity of the NSM simulations to changes in selected model parameters and (2) geographic areas in which the simulated hydrology is most sensitive to changes in model parameters. Third, results from the NSM were compared with available, but somewhat limited, historic information, on soils and vegetation.

A major, interagency effort is underway to restore significant portions of the south Florida

ecosystem and to enhance the quantity, quality, and timing of freshwater flows to the remaining Everglades. A key component of this restoration effort involves identifying hydropattern targets (primarily frequency, duration, depth, and spatial extent of water inundation) at selected key locations in the Everglades. The NSM has been proposed as the “best available tool” for estimating hydropattern targets for restoration efforts. Restoration costs may be nearly \$2 billion, and decisions made based on NSM results could have important and direct implications for the entire south Florida region.

The U.S. Geological Survey (USGS), in cooperation with the U.S. Army Corps of Engineers, Jacksonville District, conducted a study to review selected features of the NSM to determine if the NSM can provide a reasonable simulation of south Florida hydrology for pre-drainage conditions using recent climatic data. The absence of measured hydrologic, topographic, and vegetation data from the natural system for model construction and testing required that non-standard procedures be used to determine if NSM results are “reasonable.” Only selected components and features of the model were reviewed because of limited resources and time available for the review. Issues identified during discussions with staff from the SFWMD, U.S. Army Corps of Engineers, National Park Service, and Florida Department of Environmental Protection were the focus of the review, and subsequently this report (table 1).

Purpose and Scope

The purpose of this report is to document a review of selected features of the Natural System Model. Equations used to represent various components of the natural hydrologic system, along with numerical schemes used to solve the equations, were reviewed in order to clearly describe and document the manner in which processes were modeled. The effects of different temporal and spatial discretizations on model results were evaluated, and sensitivity tests were conducted using selected algorithms. Suggestions are made for appropriate uses of the NSM, based on findings from this review.

The SFWMD provided the USGS with NSM version 4.3, which was evaluated during the study by using the 1965 climatic data set also provided by the SFWMD. However, as a result of preliminary findings

Table 1. Review issues and approaches for review

Issue	Review approach
Spatial and temporal discretization.	Comparison of model results made using different computational grid cell sizes and time steps.
Spatial interpolation of precipitation data.	Review of literature and model algorithms.
Evapotranspiration computations.	Review of literature and model algorithms.
River system algorithms.	Review of governing equations, numerical solution of the equations, and model algorithms; sensitivity tests.
Overland flow algorithms.	Review of governing equations, numerical solution of the equations, and model algorithms; comparison of NSM approach with other approaches.
Ground-water system algorithms.	Review of governing equations, numerical solution of the equations, and model algorithms.
Initial and boundary conditions.	Limited review of data; review of model algorithms.
Recommended applications.	Synthesis of available information and results from reviews.

during the course of this study, revisions were made by the SFWMD to version 4.3, resulting in version 4.4. Subsequent changes may have been made in response to findings reported herein.

Previous Investigations

The primary documentation of the NSM was published by Fennema and others (1994). The report provides an overview of NSM version 3.6; an analysis of the sensitivity of model results to changes in evapotranspiration, the overland-flow resistance coefficient, and Lake Okeechobee water levels; and a comparison of NSM results to data and SFWMM simulation results. Documentation of governing equations, solution techniques, selection of model parameters, and input data were not provided. One of the first versions of the SFWMM, from which the NSM was developed, was documented by MacVicar and

others (1984). Since that time, the SFWMM has undergone numerous revisions.

Water levels and inundation periods in Water Conservation Area (WCA) 1 (fig. 2) were fairly insensitive to changes in evapotranspiration (Fennema and others, 1994). However, water levels and inundation periods in WCA 3A and at the northern end of Shark River Slough (fig. 2) were sensitive to changes in evapotranspiration. A 20-percent reduction in evapotranspiration resulted in a 73-percent increase in annual flow into Shark River Slough, and a 20-percent increase in evapotranspiration resulted in a 60-percent decrease in annual flow into the slough.

Water levels and inundation periods were generally insensitive to changes in the resistance coefficient and Lake Okeechobee water levels (Fennema and others, 1994). Flows, however, were sensitive to changes in the resistance coefficient, particularly during drier years. Flows as far south as Tamiami Trail were sensitive to changes in Lake Okeechobee water levels, with an increase of 1.5 feet (ft) in the mean lake water level resulting in 34 percent more flow at Tamiami Trail. Similar analyses for later versions of the NSM have been performed by the SFWMD staff, but have not been published, so it is not known if these results remain valid for the current version of the NSM.

Simulated water levels for the period 1980–89 were compared with measured water levels at several locations (Fennema and others, 1994). Simulated water levels and measured water levels in WCA 1 (fig. 2) exhibited fairly similar temporal patterns and differed by less than 1 ft in most months. The water-level gage in WCA 1 is in the Loxahatchee National Wildlife Refuge, which is somewhat less affected by water management activities than many other locations in south Florida. Simulated and measured water levels in the ENP also had very similar seasonal patterns, and differences between simulated and measured water levels were generally less than a foot in the western Shark River Slough and in the downstream portion of Taylor Slough (fig. 2). These results, while not a calibration of the NSM, suggest that reasonable temporal water-level patterns are simulated by the NSM in selected regions of the model domain.

Because of the absence of pre-drainage hydrologic data, the NSM simulations were qualitatively compared with available historic information to obtain a “quasi-validation” of the model.

Preliminary results (J. Obeysekera, South Florida Water Management District, written commun., August 1996) indicate that (1) simulated flow patterns are consistent with known flow patterns in the Everglades, (2) the simulated extent of inundation generally agrees with the known historic extent of the Everglades, (3) the largest simulated ground-water fluxes are to the east, consistent with historic accounts of large gradients near the Atlantic coast, and (4) simulated Lake Okeechobee levels seem to agree, in general, with historic accounts of lake levels and overflows.

An extensive analysis of historic data on soils, water depths, vegetation, and other information was conducted to reconstruct the spatial pattern of long-term average water levels and hydroperiods in south Florida for the pre-drainage period (C. McVoy, Environmental Defense Fund, written commun., 1997). The reconstructed water levels and hydroperiods were compared with simulations made using NSM version 4.4. Spatial patterns of water levels and hydroperiods from the two sets of records were in general agreement. However, long-term average annual low and high water levels simulated by the NSM were generally lower than those estimated from the historic records, with differences ranging up to 18 inches (in.). Likewise, the annual range in simulated water levels was less than the range estimated from historic records, with a simulated range of about 1 ft and a range estimated from historic records of 2 ft. Available historic records were insufficient for estimating pre-drainage flow volumes. Interannual variations in high and low water levels were not determined, but limited information indicated that variations of up to 1 ft around the long-term average might have been common. It is important to note, however, that soils and, to a lesser extent, vegetation integrate the effects of centuries of climatic and hydrologic variability, whereas NSM version 4.4 simulates pre-drainage hydrologic response based on about 25 years of recent climatic data.

Loucks and Stedinger (1994) addressed the issues of sensitivity analysis and uncertainty in the SFWMM and the NSM. The variability and uncertainty in model output was determined to be a function of model inputs, parameter values, initial and boundary conditions, and model structure, including numerical solution techniques. Loucks and Stedinger noted that parameter and model uncertainties become more important when the model is used to extrapolate

beyond conditions that have been observed. Several recommendations were made concerning approaches for conducting sensitivity and uncertainty analyses for the SFWMM and the NSM. Loucks and Stedinger also recommended that automated model calibration routines be developed for objective model calibration and better determination of statistical properties of model parameters.

In response to the report by Loucks and Stedinger (1994), Trimble (1995) conducted an investigation to (1) identify the most feasible methods for evaluating the sensitivity of and uncertainty in the SFWMM and (2) apply one or more of the methods to estimate uncertainty associated with selected SFWMM performance measures. Although Trimble's study addressed the SFWMM, results from the investigation are relevant to the NSM because the NSM parameters are derived from the SFWMM calibrations. Trimble noted that, "only a small amount of information exists documenting the reasonable ranges for several [SFWMM] parameters."

Trimble (1995) concluded that there was no region of the model domain which was insensitive to changes in at least one of the model parameters. Potential evapotranspiration dominates all other processes, and evapotranspiration parameters cannot be changed more than 5 percent without degrading the model calibration. Changes in evapotranspiration resulting from parameter adjustments appeared to be balanced by changes in flow.

Water levels in all regions of the model except the ENP, where overland flow is the dominant flow process, were insensitive to changes in the Manning n . Trimble (1995) suggested that use of the Manning relation (which relates water velocity to flow resistance, channel geometry, and channel slope) might not be acceptable for simulating overland flow for 2-mi by 2-mi computational cells in which secondary flow channels are present, and in which significant water-level differences can occur, particularly near the east coast. (Canals are not present in the NSM.) However, Trimble noted that because the SFWMM is used as a water-balance model rather than a flow-routing model, application of the Manning relation may be acceptable.

Trimble (1995) concluded that model parameter uncertainty in the SFWMM is much less than the total uncertainty in the model. Much of the model

uncertainty, according to Trimble, can be associated with rainfall amounts and flows at control structures.

Additional sensitivity analyses were performed by SFWMD staff (J. Obeysekera, South Florida Water Management District, written commun., January 1995). The evapotranspiration crop coefficients and Manning n -values were varied, and NSM results were analyzed using a sensitivity matrix. Simulated results were most sensitive to changes in evapotranspiration coefficients and less sensitive to changes in the resistance coefficient. Similar results were reported by Fennema and others (1994). Results were most sensitive to changes in evapotranspiration coefficients in the central region of the model domain (A.M.W. Lal, South Florida Water Management District, written commun., January 1997). A change of 1 ft in the topographic elevation at the southern rim of Lake Okeechobee had a significant effect on simulated flows in the model domain. A change in the evapotranspiration coefficient in one computational cell was found to affect simulated results for a distance of about 5 cells away from the cell in which the change was made.

The simulated flow patterns presented by Fennema and others (1994) exhibited some unusual features. Specifically, velocities along the western boundary of the model were significantly greater than those just to the east of the boundary (fig. 3). Likewise, there was a region of high velocities near the northern boundary of the model domain. Flows at the boundaries were generally parallel to the boundary, and were to the east at the northern boundary and to the south at the western boundary. These flow patterns were not discussed in the report. Similar results were seen in NSM version 4.2 simulations (J. Obeysekera, South Florida Water Management District, written commun., January 1995).

Van Lent and others (1993) used NSM version 3.6 to compare pre- and post-drainage flows in the lower Taylor Slough Basin (fig. 2). The authors noted that the 2-mi by 2-mi computational grid size limited the usefulness of NSM results in small regions, such as Taylor Slough. Additional uncertainty in the Taylor Slough simulations was introduced by the proximity of Taylor Slough to the model boundary, where boundary conditions are estimated. Among the recommendations of Van Lent and others, it was noted that water levels, rather than flows, are the key indicator of marsh restoration.

Van Lent (1995) developed a linear stochastic model for relating water levels in Shark River Slough (fig. 2) to rainfall and potential evapotranspiration. Rainfall alone was found to be a reasonable predictor of Shark River Slough water levels, but the linear model appeared to inadequately replicate the inundation patterns in the slough. Van Lent also concluded that wet season and dry season water-level fluctuations in the Shark River Slough are controlled by different physical processes.

A two-dimensional hydrodynamic model was developed for a 3,815-acre Stormwater Treatment Area (STA) located in the northwest corner of WCA 1 (fig. 2) (Guardo and Tomasello, 1995). The STA is about the size of 1.5 NSM computational cells. Vegetation in the model domain is primarily cattails, mixed macrophytes, submerged macrophytes and algae; this vegetation is like vegetation in much of the NSM domain. The model consisted of 600 computational cells, 600 ft by 906 ft. A Manning formulation was used to describe flow resistance; the Manning n -value was set to 1.0 in the model. Simulated flow velocities ranged from 0.0012 to 0.015 foot per second (ft/s) for inflows ranging from 75 cubic feet per second (ft³/s) to 600 ft³/s. Manning n -values in the NSM range from about 0.04 to more than 2.0, depending on vegetation type and water depth. These differences in Manning n -values demonstrate the effects of grid size and model formulation on the n -value used in a particular model.

Abtew and others (1993) evaluated six methods for estimating point and areal rainfall in a 4,000-mi² area of inland south Florida where 25 raingages were located. The optimal interpolation and kriging methods provided good estimates of monthly point and areal rainfall throughout the study area. In contrast, the NSM daily rainfall in ungaged computational cells (cells representing areas where no raingage is present) is assumed to be equal to the measured rainfall at the nearest raingage. This approach can lead to discontinuities in rainfall when two adjacent computational cells obtain rainfall estimates from two different raingages. In addition, most of the 485 raingages from which the NSM data are obtained are concentrated along the east coast of south Florida. Annual average rainfall in the model domain ranges from about 35 to 65 in., with higher values occurring primarily along the east coast.

Chin and Zhao (1995) used global error variance to, among other things, identify the best method for

estimating reference-crop evapotranspiration (evapotranspiration from a vegetative surface) in south Florida. Global error variance was estimated from evaporation-pan networks and empirical evaporation equations (Penman-Monteith, Blaney-Criddle, and Stephens-Stewart) based on meteorological data-collection networks in the SFWMD, which roughly coincide with the NSM domain. Chin and Zhao concluded that universal kriging provided better estimates of reference-crop evapotranspiration in south Florida than the three empirical equations. They attributed this to the fact that accurate measurements of meteorological parameters, which are required for the empirical equations, are generally unavailable and must be estimated from remote meteorological stations. Of the three empirical functions evaluated, the Penman-Monteith function was found to provide the best estimates of reference-crop evapotranspiration in south Florida. The Penman-Monteith method is used for estimating reference evapotranspiration in the NSM, and an inverse-distance weighting scheme is used for the spatial distribution of the evapotranspiration values.

Bidlake and others (1993) evaluated three micrometeorological methods for estimating evapotranspiration from dry prairies, marshes, pine flatwoods, and cypress swamps in west central Florida. Calculated annual evapotranspiration values during the study period were 39.8 in. (dry prairie), 39.0 in. (marsh), 41.7 in. (pine flatwoods), and 38.2 in. (cypress swamp). Bidlake and others found that evapotranspiration was about 57 percent of potential evapotranspiration at the marsh site. Potential evapotranspiration calculation methods, such as the Penman-Monteith method, were found to be unsuitable for estimating evapotranspiration from pine flatwood and cypress swamp sites. However, potential evapotranspiration methods might be appropriate for marsh vegetation.

Potential evapotranspiration varied seasonally (Bidlake and others, 1993). The 3 months of lowest average potential evapotranspiration at the dry prairie sites were November, December, and January, and the highest potential evapotranspiration was during March through June. Similar seasonal variations likely occurred for the other vegetation types.

Acknowledgments

The assistance, technical guidance, and open discussions provided by M. Choate, U.S. Army

Corps of Engineers, Jacksonville District; A. Lal, C. Neidrauer, J. Obeysekera, and R. Van Zee, South Florida Water Management District; and R. Fennema, Everglades National Park, are gratefully acknowledged. E. Hayter, Clemson University, ably performed the comparison of NSM results with simulations from a two-dimensional hydrodynamic model. L. DeLong, U.S. Geological Survey (retired), contributed to the initiation and planning of this investigation.

GOVERNING EQUATIONS AND BOUNDARY CONDITIONS

The basic equation solved by the NSM is conservation of mass. This equation can be expressed as a summation of the changes in volume of the various hydrologic systems as

$$\frac{\partial V_T}{\partial t} = \frac{\partial V_r}{\partial t} + \frac{\partial V_o}{\partial t} + \frac{\partial V_{gw}}{\partial t}, \quad (1)$$

where

V_T is the total water volume in the NSM,

V_r is the water volume associated with the river systems,

V_o is the water volume associated with the overland-flow system,

V_{gw} is the water volume associated with the ground-water system, and

t is time.

Because the surface areas of each system (river, overland flow, and ground-water flow, respectively) are considered constant, equation 1 can be expressed as

$$\frac{\partial V_T}{\partial t} = A_r \frac{\partial Y_r}{\partial t} + A_o \frac{\partial H}{\partial t} + A_{gw} \frac{\partial h}{\partial t}, \quad (2)$$

where

Y_r is the river stage or water-surface elevation for the river system,

H is the overland-flow ponding depth,

h is the ground-water elevation relative to an arbitrary datum, and

$A_r, A_o,$ and A_{gw} are the surface areas of the river, overland-flow, and ground-water systems, respectively.

Equation 2 is a relatively simple partial differential equation. However, each term on the right side of the equation represents a complex hydrologic system, requiring the use of additional equations to compute the values for each of these terms. The following three sections present, in detail, the equations solved by the NSM that represent each of the hydrologic systems—river, overland flow, and ground water—described by the terms on the right side of equation 2.

The partial differential equations are solved in the NSM by using finite-difference techniques. Finite-difference techniques require the subdivision of the solution domain into a grid with a finite number of node points. Continuous derivatives at each point are then replaced by a finite-difference approximation to the derivative. The NSM uses a 41- by 80-node grid to represent the solution domain (fig. 3). Each node represents a 2-mi by 2-mi cell (fig. 3) and is assigned a particular land-use type which reflects the general vegetation, soil type, and flow roughness in the cell. Equations that represent the hydrologic system are then solved for each node and associated cell.

The hydrologic processes that are included within each cell in the NSM, or the intracell hydrologic processes, are precipitation, evapotranspiration, seepage or recharge between the river and ground-water systems, seepage or infiltration from the overland-flow system to the ground-water system, flow from the ground-water system to the overland-flow system, and flow between the overland and river systems. The hydrologic processes represented between cells are ground-water, overland, and river flow. These processes are represented in the governing equations described in the following sections. The effects on flow of solar heating, inertia, rotation of the Earth, and wind are considered negligible for this system and are not included in the governing equations.

For each computational time step, the order of solution is (1) the river system, (2) the overland-flow system, and (3) the ground-water system. Prior to the solution of the river system, precipitation is added to the ponding depths at each node and to river stage throughout the grid. After the solution of the ground-water system, the water-surface elevations in nodes that represent lake land-use types are equalized so that the water-surface elevations are the same for each lake node, resulting in a level lake surface.

River-System Flow Equations

The NSM uses a simplified flow equation to represent river systems. River properties for the appropriate river segment, such as flow length and surface area, are assigned to a node if a river segment lies within the domain of the node (or cell). The equation solved for each river system is

$$\frac{\partial V_r}{\partial t} = Q_f + R_r - Q_r + P_r - E_r, \quad (3)$$

where

V_r is the volume of water in a river,

Q_f is flow between the river system and the overland-flow system,

R_r is the flow between the river system and the ground-water system (or seepage),

Q_r is the flow into and out of the ends of the river segment in the cell,

P_r is the precipitation directly on the river, and

E_r is evaporation from the river.

This solution technique is similar to storage routing techniques described in many hydrology texts (for example, Linsley and others, 1975). Twenty-nine distinct river systems are included in the NSM domain.

Equation 3 is expressed for each river system as a forward-in-time finite-difference formulation:

$$A_r Y_{t+1} = A_r Y_t + (Q_f + R_r - Q_r - E_r) \Delta t, \quad (4)$$

where V_r is replaced by the product of the surface area of the individual river system, A_r , and the stage, Y ; Y_r is replaced by Y for clarity; and the subscripts t and $t+1$ refer to the present and subsequent computational time steps, respectively. Precipitation is implicit in equation 4 because it is added to the river stage prior to the solution of equation 4. Because the terms on the right side of equation 4 are dependent on Y_{t+1} , an iterative method similar to the bisection technique (Conte, 1980) is used to solve the equation.

The intracell flow between a river and the overland system is computed as

$$Q_f = \sum_{m=1}^M \frac{1.49}{n_m} \left[|(H_{m,t} + Z_m) - (Y_{t+1} + f_m)| \frac{4}{\Delta x} \right]^{\frac{1}{2}} \times \left(\Gamma_{m,t+1}^{\frac{5}{3}} L_m \right), \quad (5)$$

where

f_m is the fall in the water surface of the river,

H_m is the ponding depth,

Z_m is the land-surface elevation,

L_m is the distance to the river node measured from the downstream end of the river system (fig. 4), and

$\Gamma_{m,t+1}$ is a flow depth the definition of which is a function of flow conditions, as explained subsequently.

The subscript, m , represents a river-system node and its associated river segment. Each of the river nodes corresponds to one of the i,j cell nodes in the 41- by 80-node grid. M is the total number of nodes in a river system. The roughness term, n_m , is computed as $n_m = a\Gamma_m^b$, where a and b are constants associated with a river system. These constants are part of the NSM input data and are $a=3.0$ and $b=0$. These values result in $n=3.0$. The fall is computed at each node as

$$f_m = F_r \left(1 - \frac{(L_r - L_m)}{L_r} \right), \quad (6)$$

where F_r is the change in water-surface elevation over the entire river system, and L_r is the total length of the river system. F_r is constant with time for a river system and is defined in the input data.

If $[(H_{m,t} + Z_m) - (Y_{t+1} + f_m)]$ is less than zero (flow out of the river into the overland system), then Γ_m is an area-weighted flow depth, or

$$\Gamma_{m,t+1} = [a_m(Y_{t+1} + f_m - Z_m) + H_{m,t}(\Delta x \Delta y - a_m)] \div (\Delta x \Delta y), \quad (7)$$

where a_m is the surface area of the river associated with the m river node. If $[(H_{m,t} + Z_m) - (Y_{t+1} + f_m)]$ is greater

than zero (flow into the river from the overland system), then Γ_m is equal to the ponding depth in the grid cell associated with that river segment, or

$$\Gamma_{m,t+1} = H_{m,t}. \quad (8)$$

Flow out of the overland system into the river is limited to be less than or equal to the available water volume in the cell above the detention depth, or

$$Q_f \leq (H_m - \delta_m) \Delta x \Delta y, \quad (9)$$

where δ_m is the detention (or surface storage) depth and is defined in the input data set as a function of land-use type. However, no limit is placed on the flow out of the river into the overland system, on seepage from the river to the ground-water system, or on evaporation from the river system. This means that, as presently configured in the NSM, the solution of equation 4 does not guarantee mass conservation. Tests were not conducted to determine if mass conservation was actually violated during application of the NSM. Most of the water in the NSM domain is not in the river systems, but in the overland-flow and ground-water systems. Consequently, the failure to ensure mass conservation in the NSM river system probably has little effect on the simulation of water levels and hydroperiod in the Everglades region of the NSM domain.

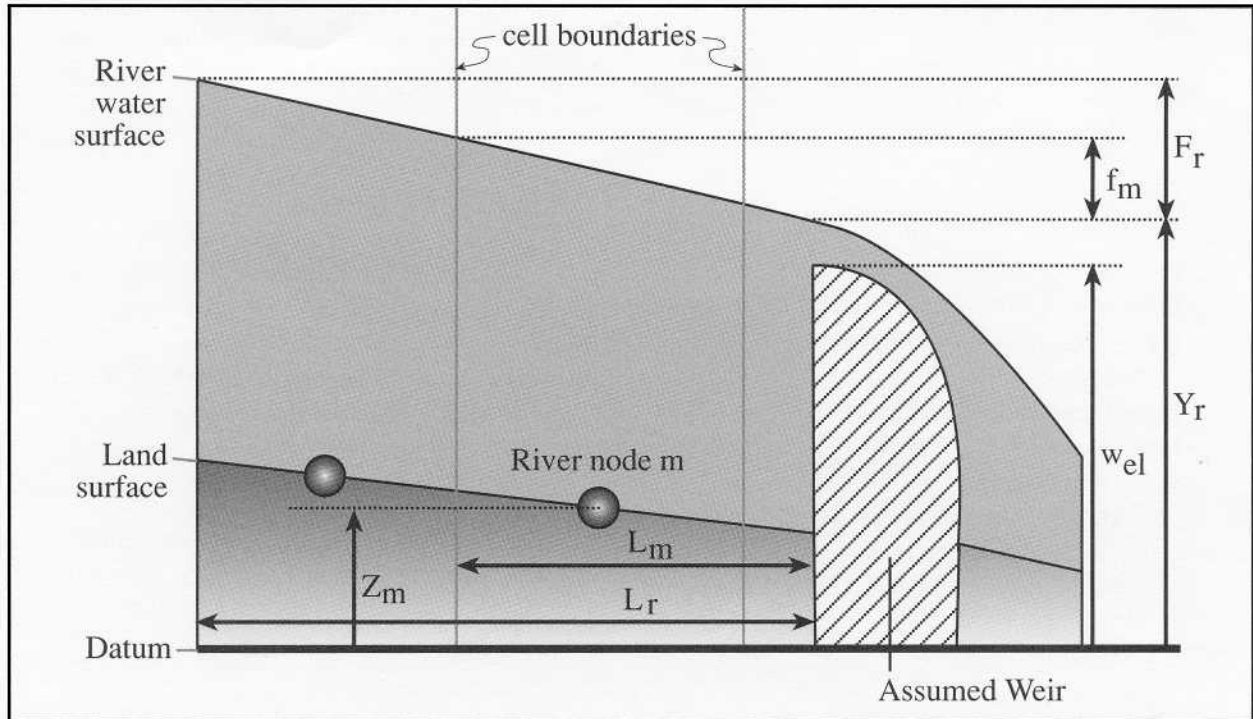
The flow between the river and ground-water system, or seepage, is computed as

$$R_r = 1.4 \sum_{m=1}^M K_m (Y_{t+1} + f_m - h_{m,t}) a_{i,j}, \quad (10)$$

where M is the total number of river nodes in a river system, h_m is the ground-water elevation at the m river node, 1.4 is an adjustment to $a_{i,j}$, which is the surface area of the river at node i,j , and K_m is a river seepage coefficient, in feet per day per foot of head, for the m river node that is defined in the input data.

The flow into and out of the river system for each computational time step is determined from an inflow value supplied by the input data and an outflow value

A



B

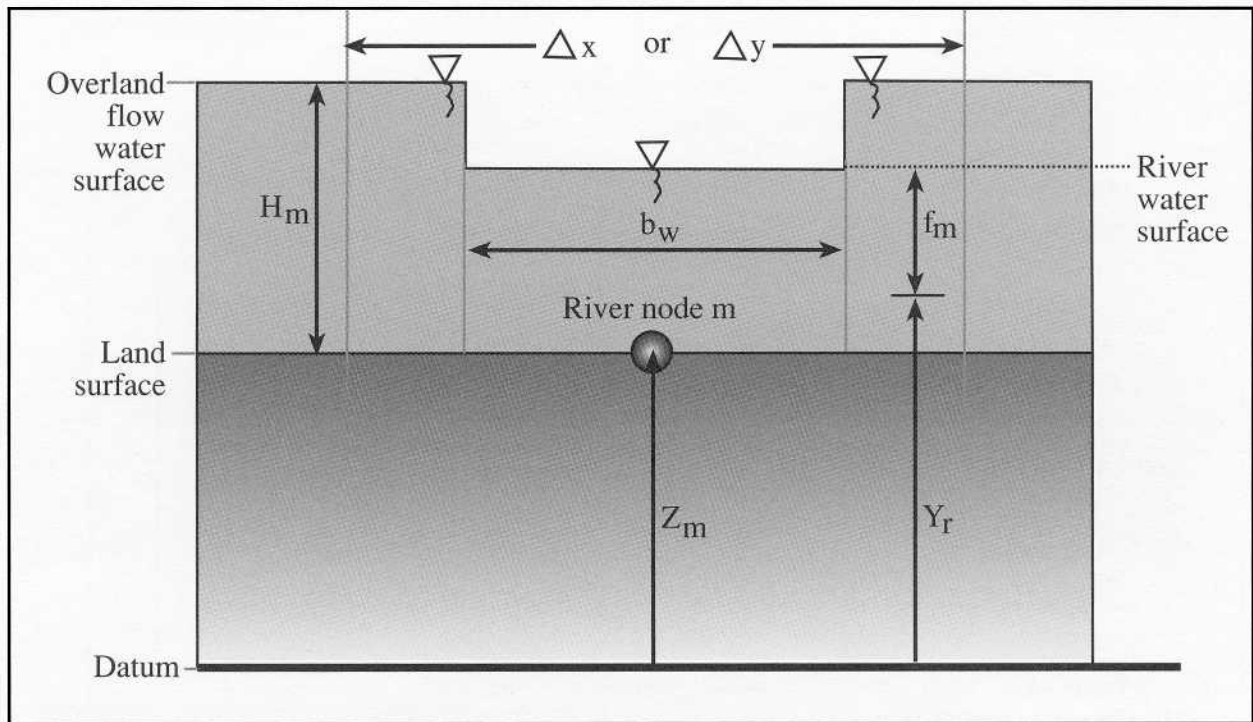


Figure 4. Variables used in the river-system equation. (A) Longitudinal view along the length of a river system, and (B) Side view of a cell within a river segment.

computed using a weir equation. The resulting equation is

$$Q_r = k_w b_w (Y_{t+1} - w_{el}) [2g(Y_{t+1} - w_{el})]^{1/2} - q_{t+1}, \quad (11)$$

where

- k_w is a weir coefficient,
- g is the acceleration of gravity,
- q_{t+1} is the river-system inflow specified in the input data set at the $t+1$ time step,
- b_w is the width of the weir, and
- w_{el} is the elevation of the weir crest.

Both b_w and w_{el} are estimates for each river system and are defined as part of the input data.

Evapotranspiration from the river system is computed as

$$E_r = \sum_{m=1}^M Emax_m e_m, \quad (12)$$

where $Emax_m$ is the maximum evapotranspiration coefficient which is specified in the input data as a function of land-use type. e_m is the potential evaporation computed for each node from input values of zone potential evapotranspiration, adjusted by input node station weights.

Overland Flow

The overland-flow system is simulated by using a simplified two-dimensional flow equation. The governing equation, numerical solution of the equation, and boundary conditions applied in the solution of the equation are presented in this section.

Equations

The NSM uses a simplified two-dimensional flow equation to represent overland flow. The basic overland-flow equation for each cell is the conservation of mass (fig. 5):

$$A_o \frac{\partial H}{\partial t} = -I_o - E_o + Q_f + P_o + Q_{gw} - Q_o, \quad (13)$$

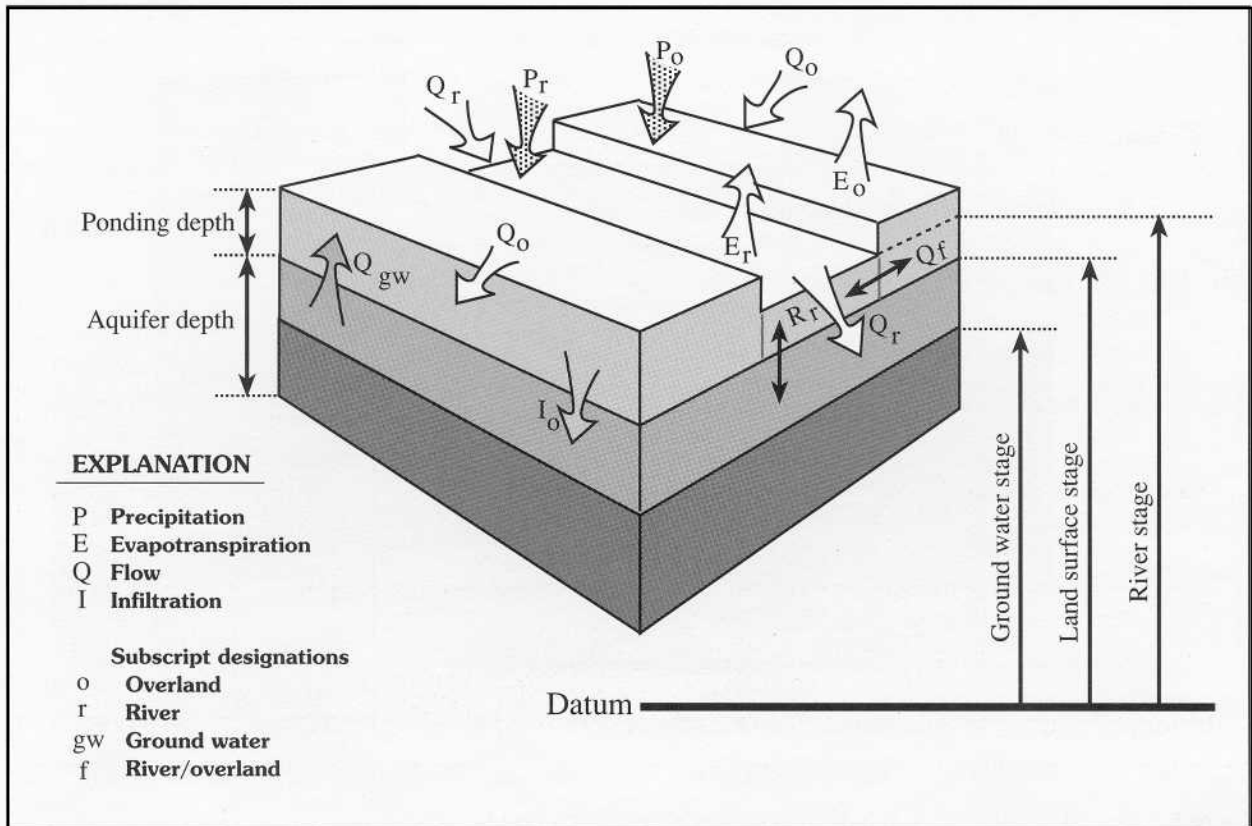


Figure 5. Intracell and intercell hydrologic processes represented within the Natural System Model.

where

I_o is infiltration to the ground-water system,

E_o is the evapotranspiration from the overland-flow system,

H is the water depth (or ponding depth),

Q_f is the flow between the river and overland systems,

P_o is the precipitation,

Q_{gw} is the flow from the ground-water system to the overland system,

and Q_o is the exchange of overland flow between cells.

Although the overland-flow system includes the effects of precipitation, flow between the river and overland system (fig. 6), and flow from the ground-water system, these processes are not explicitly computed in the equations solved for overland flow. Only the exchange of overland flow between cells, infiltration, and evapotranspiration are explicitly computed. Precipitation is added to all ponding depths at the beginning of a time step. The exchange of flow between overland and river systems is simulated during

the river-system computations (eq. 5), and flow from the ground-water system is simulated as part of the ground-water equations. Thus, the equation used is

$$\frac{\partial H}{\partial t} + \frac{\partial Hu}{\partial x} + \frac{\partial Hv}{\partial y} = -I_o - E_o, \quad (14)$$

where the overland flow between cells is represented by the second and third terms on the left side of the equation, u is the overland-flow velocity in the x -direction, and v is the overland-flow velocity in the y -direction.

This equation is discretized by using a simple forward difference in time. Infiltration and evapotranspiration are computed in two separate steps after the computation of overland flow between cells. The technique used to solve the equation is similar to storage routing techniques described by Linsley and others (1975) for one-dimensional flow systems, but is applied to a two-dimensional system in the NSM.

The NSM solves for the exchange of water volumes by overland flow through two of the four sides

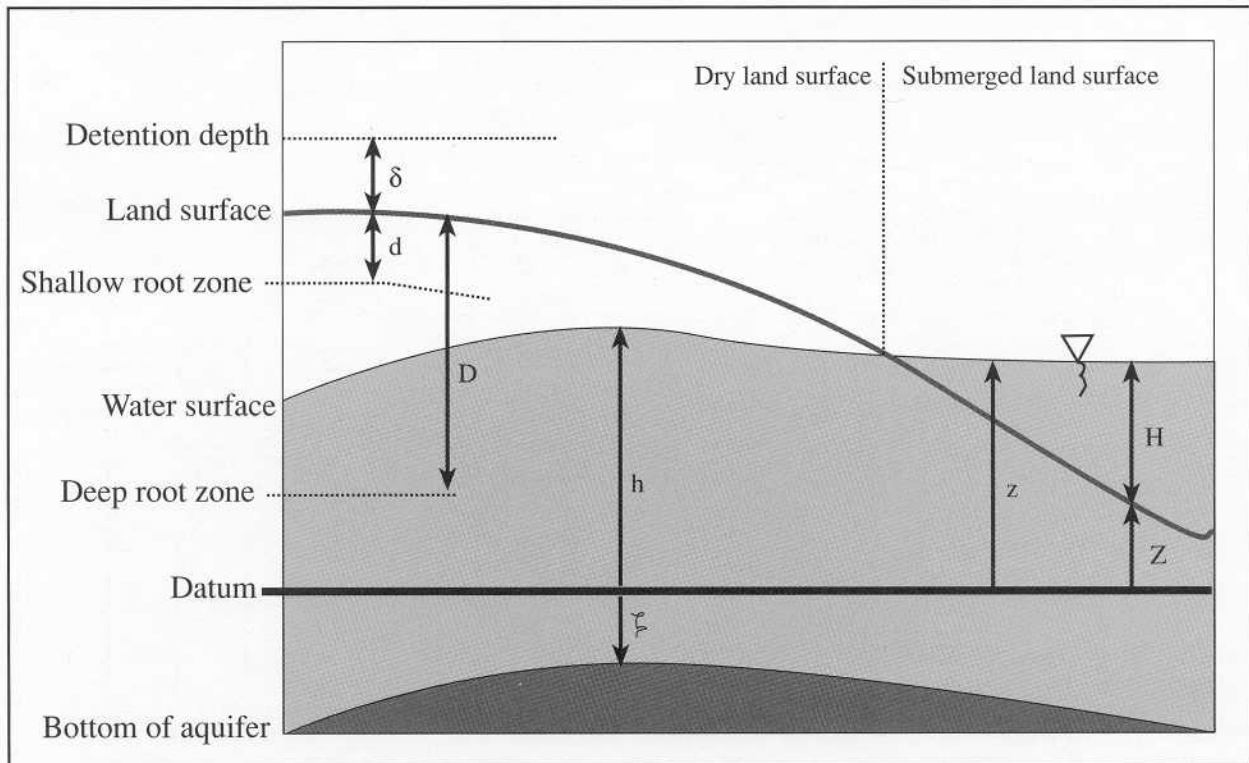


Figure 6. Overland and ground-water flow variables in the Natural System Model.

of a computational cell. The grid is solved in alternating directions (east to west and south to north, and west to east and north to south) to improve solution convergence and to minimize possible solution bias that may occur if the solution proceeded in the same direction for each time step. Information from the current cell (the one for which a solution is desired) and from two adjacent cells, either the cells to the east and south, or the cells to the north and west of the current cell, is used to solve the equations. Mass is balanced over the three cells represented by the three nodes that are used to compute flow through the two cell sides. Ponding depths are computed for the current node at the new time step and are updated with intermediate values at the two adjacent nodes used in computing depth at the current node. This results in two iterations for the solution at a node, one when the node is not the current node and the other when it is.

The numerical method used in the solution of the overland-flow equation is asymmetric and explicit. This results in two equations that are solved for ponding depth, with one equation used for each computational direction. For a computation proceeding from west to east and north to south across the grid (fig. 7A), equation 14 is discretized and solved for

ponding depths at the current node at the new time step as

$$H_{i,j,t+1} = H_{i,j,t} - \left[u_{i+\frac{1}{2},j,t+1} H_{i+\frac{1}{2},j,t} \left(\frac{\Delta t}{\Delta x} \right) - \left[v_{i,j-\frac{1}{2},t+1} H_{i,j-\frac{1}{2},t+1} \left(\frac{\Delta t}{\Delta y} \right) \right] \right] \quad (15)$$

The ponding depths at the two adjacent nodes are updated with intermediate values as

$$H_{i+1,j,t^*} = H_{i+1,j,t} + u_{i+\frac{1}{2},j,t} H_{i+\frac{1}{2},j,t} \left(\frac{\Delta t}{\Delta x} \right) \quad (16)$$

and

$$H_{i,j-1,t^*} = H_{i,j-1,t} + v_{i,j-\frac{1}{2},t} H_{i,j-\frac{1}{2},t} \left(\frac{\Delta t}{\Delta y} \right), \quad (17)$$

where t^* denotes an intermediate computation that occurs between t and $t + 1$.

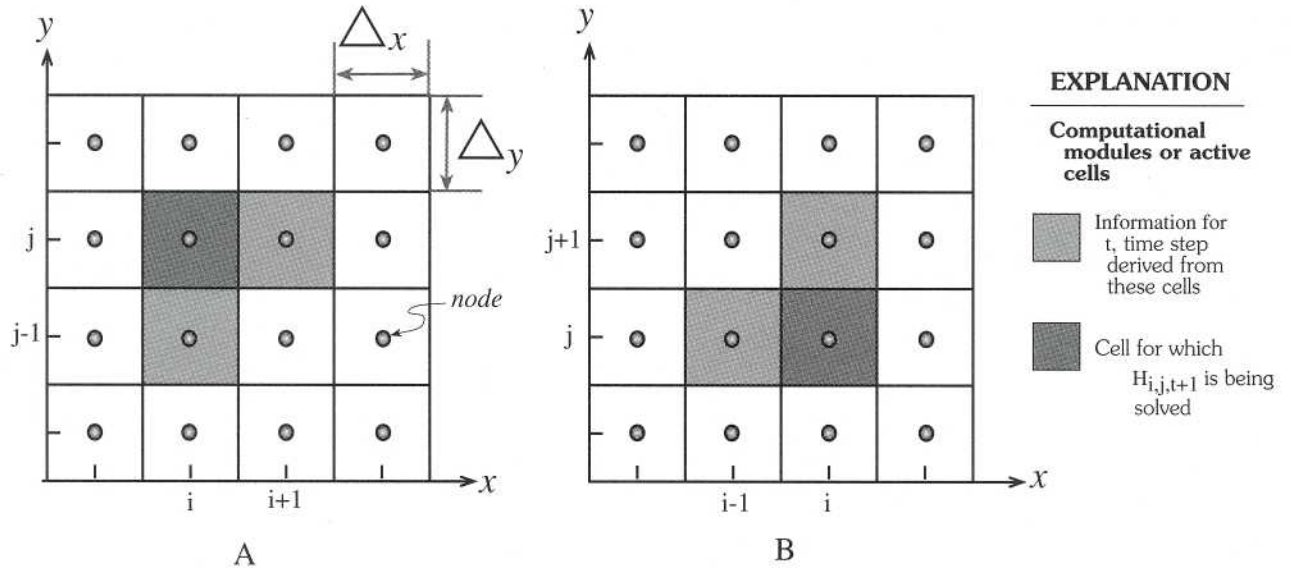


Figure 7. Computational modules or active cells in a grid fragment for solution of overland flow between cells for calculations for $H_{i,j,t+1}$ proceeding from (A) west to east and north to south, and (B) east to west and south to north.

For east to west and south to north computations across the model grid (fig. 7B), the equation for the current node at the new time step is

$$H_{i,j,t+1} = H_{i,j,t} - \left[u_{i-\frac{1}{2},j,t+1} H_{i,j-\frac{1}{2},t} \left(\frac{\Delta t}{\Delta x} \right) \right] - \left[v_{i,j+\frac{1}{2},t+1} H_{i,j+\frac{1}{2},t} \left(\frac{\Delta t}{\Delta y} \right) \right]. \quad (18)$$

For the intermediate ponding depths at the adjacent nodes, the equations used are

$$H_{i-1,j,t^*} = H_{i-1,j,t} + u_{i-\frac{1}{2},j,t} H_{i-\frac{1}{2},j,t} \left(\frac{\Delta t}{\Delta x} \right) \quad (19)$$

and

$$H_{i,j+1,t^*} = H_{i,j+1,t} + v_{i,j+\frac{1}{2},t} H_{i,j+\frac{1}{2},t} \left(\frac{\Delta t}{\Delta y} \right). \quad (20)$$

The subscripts i, j denote the location of the computed node in the grid, t is the time step, Δx is the grid spacing in the x -direction, Δy is the grid spacing in the y -direction, and Δt is the time-step size.

Finite difference schemes typically align the computational module so that the unknown node lies in the interior of the grid and the known nodes lie on the grid boundaries. Boundary conditions at the new time step can then be used to solve for the unknown node at the new time step with no intermediate updating between the t and $t+1$ time step. The computational modules for equations 5 and 18 (fig. 7) are not aligned with the known values on the boundaries. Instead, the determination of the values at the unknown boundary node at time $t+1$ is a function of the type of boundary condition which has been established. Values at the adjacent nodes are then updated at an intermediate time step, t^* , by using equations 19 and 20. This intermediate updating allows the boundary conditions to be transmitted into the grid even though the unknown node is also the boundary condition node.

The velocity terms (u and v) in equations 15 and 18 are computed from the uniform flow, or Manning, equation. The form of the Manning equation used in the NSM can be derived from the two-dimensional

momentum equation, which describes the forces represented in the NSM overland-flow equation. The two-dimensional depth-averaged equations for conservation of momentum are

$$\frac{\partial(Hu)}{\partial t} + \frac{\partial(Huu)}{\partial x} + \frac{\partial(Huv)}{\partial y} + gH \frac{\partial Z}{\partial x} + \frac{g}{2} \frac{\partial H^2}{\partial x} \quad (21)$$

$$- \Omega H v + \frac{1}{\rho} \left[\tau_{b,x} - \tau_{s,x} - \frac{\partial H \tau_{xx}}{\partial x} - \frac{\partial H \tau_{xy}}{\partial y} \right] = 0$$

and

$$\frac{\partial(Hv)}{\partial t} + \frac{\partial(Hvu)}{\partial x} + \frac{\partial(Hvv)}{\partial y} + gH \frac{\partial Z}{\partial y} + \frac{g}{2} \frac{\partial H^2}{\partial y} \quad (22)$$

$$- \Omega H u + \frac{1}{\rho} \left[\tau_{b,y} - \tau_{s,y} - \frac{\partial H \tau_{yx}}{\partial x} - \frac{\partial H \tau_{yy}}{\partial y} \right] = 0,$$

where

g is acceleration of gravity,

Ω is Coriolis parameter,

ρ is water density,

Z is land-surface elevation,

$\tau_{b,x}$ and $\tau_{b,y}$ are bed shear stresses acting in the x - and y -directions, respectively,

$\tau_{s,x}$ and $\tau_{s,y}$ are surface shear (wind) stresses acting in the x - and y -directions, respectively,

and τ_{xx} , τ_{xy} , τ_{yx} , and τ_{yy} are shear stresses caused by turbulence.

If the acceleration, momentum fluxes (first three terms on the left of eqs. 21 and 22), Coriolis, wind stress, and turbulence terms are assumed to be negligible, the momentum equations are reduced to

$$gH \frac{\partial Z}{\partial x} + \frac{g}{2} \frac{\partial H^2}{\partial x} + \frac{1}{\rho} \tau_{b,x} = 0 \quad (23)$$

and

$$gH \frac{\partial Z}{\partial y} + \frac{g}{2} \frac{\partial H^2}{\partial y} + \frac{1}{\rho} \tau_{b,y} = 0. \quad (24)$$

The bed shear-stress terms in equations 23 and 24 can be formulated using the Manning equation to give

$$\tau_{b,x} = \tau_b \cos(\alpha) = gn^2 \rho \frac{u\sqrt{uu+vv}}{cH^{1/3}} \quad (25)$$

and

$$\tau_{b,y} = \tau_b \cos(\beta) = gn^2 \rho \frac{v\sqrt{uu+vv}}{cH^{1/3}}, \quad (26)$$

where

n is Manning coefficient,

c is a constant to maintain proper unit conversion,

α is the flow angle with respect to the x -axis, and

β is the flow angle with respect to the y -axis.

Substituting equations 25 and 26 into equations 23 and 24, respectively, yields

$$H \frac{\partial Z}{\partial x} + H \frac{\partial H}{\partial y} + \frac{1}{\rho} \left[\rho n^2 \frac{(u\sqrt{uu+vv})}{cH^{1/3}} \right] = 0 \quad (27)$$

and

$$H \frac{\partial Z}{\partial y} + H \frac{\partial H}{\partial x} + \frac{1}{\rho} \left[\rho n^2 \frac{(v\sqrt{uu+vv})}{cH^{1/3}} \right] = 0. \quad (28)$$

Foot-second units are used in the NSM, so $c = 1.49$.

Rearranging equations 27 and 28, solving for u and v , and defining $[\partial Z/\partial x + \partial H/\partial x] = \partial z/\partial x$ and $[\partial Z/\partial y + \partial H/\partial y] = \partial z/\partial y$, where $z =$ water-surface elevation when $z > Z$ (land surface is submerged; fig. 6), the forms of the momentum equations solved by the NSM are

$$u = \frac{1.49}{n} H^{2/3} \sqrt{\cos(\alpha) \frac{\partial z}{\partial x}} \quad (29)$$

and

$$v = \frac{1.49}{n} H^{2/3} \sqrt{\cos(\beta) \frac{\partial z}{\partial y}}. \quad (30)$$

The NSM uses water-surface slope to determine the angle of the flow relative to the grid axis. For the computational module represented in figure 7A, the cosine (α) term in equation 29 is computed as

$$\cos(\alpha) = \frac{|z_{i,j,t} - z_{i+1,j,t+1}|}{\sqrt{(z_{i,j,t} - z_{i+1,j,t+1})^2 + (z_{i,j,t} - z_{i,j-1,t+1})^2}} \quad (31)$$

The cosine (β) term in equation 30 is the same as $\cos(\alpha)$ in equation 31, except that the numerator in equation 31 becomes $|z_{i,j,t} - z_{i,j-1,t+1}|$.

The simplified momentum equations (eqs. 29 and 30) are solved for computations proceeding from west to east and north to south (fig. 7A) for the current time step, $t+1$, in the following forms:

$$u_{i,j,t+1} = \frac{1.49}{n_{i,j}} \left(\frac{(H_{i,j,t} + H_{i+1,j,t+1})}{2} \right)^{2/3} \times \left(\sqrt{\frac{\cos(\alpha_t) |z_{i,j,t} - z_{i+1,j,t+1}|}{\Delta x}} \right) \quad (32)$$

and

$$v_{i,j,t+1} = \frac{1.49}{n_{i,j}} \left(\frac{(H_{i,j,t} + H_{i,j-1,t+1})}{2} \right)^{2/3} \times \left(\sqrt{\frac{\cos(\beta_t) |z_{i,j,t} - z_{i,j-1,t+1}|}{\Delta y}} \right). \quad (33)$$

Flow direction for the velocities is determined from the sign of the difference terms enclosed in the absolute value signs in equations 32 and 33. A set of equations analogous to equations 32 and 33 is solved for computations proceeding from east to west and south to north (fig. 7B).

The Manning coefficient used in equations 32 and 33 (and for the analogous equations for computations proceeding in the east to west and south

to north directions) is for the i,j node. The coefficient is computed from $n_{i,j} = aH_{i,j,t}^b$, where a and b are constants associated with a land-use type in the i,j node; these constants are part of the input data, with $0.04 < a < 1.45$. Superscript b may be either -0.77 (resistance increases with decreasing flow depth) or 0 (resistance is constant with depth). Yet, velocities are computed from information in the adjacent nodes as well as in the i,j node (eqs. 32 and 33; fig. 7). Consequently, the n -value used to compute the velocities would be more representative of the average roughness along the flow path if a length-weighted coefficient was computed from the roughness in the same nodes as those used in the velocity computation. The use of length-weighted n -values would also ensure that consistent n -values are used in the computations, regardless of the computational direction. Only velocities in nodes which are at the interface of land-use types would be directly affected by this algorithm change, although the effects of these changes would propagate throughout the entire model domain.

Simulation results from explicit numerical methods, such as the method used in the NSM to solve the overland-flow equations, are sensitive to the size of the computational time step. Numerical instabilities can occur in the solution of the overland-flow equation if the simulated velocity in a particular computational cell exceeds the ratio of the grid spacing to the time step. These instabilities occur because the computations propagate flow through more than one computational cell in a single computational time step. The NSM includes an algorithm to maintain numerical stability, by limiting the volume of water that can pass from one cell node in a single computational time step to

$$u\Delta t\Delta x\left(\frac{H_{i+1,j,t} + H_{i,j,t}}{2}\right) \leq \Delta x\Delta x\left(\frac{z_{i+1,j,t} - z_{i,j,t}}{2}\right). \quad (34)$$

A similar limiting function exists for the y -direction. This limiting function, however, affects the proper selection of the computational time and space step because equation 34 limits the maximum water velocity that can occur in the grid.

Infiltration and evapotranspiration are computed after the exchange of overland flow between cells is computed. The infiltration term, $I_{i,j,t+1}$, is computed

when the ponding depth at a node is greater than zero ($H_{i,j,t} > 0$) as

$$I_{i,j,t+1} = S_s(z_{i,j,t} - h_{i,j,t}), \quad (35)$$

where S_s is the input soil storage coefficient and $h_{i,j,t}$ is the elevation of the ground-water surface, which is limited to be less than or equal to the land-surface elevation (see following section). Infiltration is limited to be less than or equal to the ponding depth ($I_{i,j,t} \leq H_{i,j,t}$). Infiltration is added to the recharge term, R_{gw} , of the ground-water flow equation and is subtracted from the ponding depth.

The overland-flow system evapotranspiration, E_o , is dependent on land-use type, ponding depth, and the ground-water elevation at the node. For nodes that have ponding depths greater than the open-water ponding depth, $O_{i,j}$ (or $H_{i,j,t} > O_{i,j}$), E_o is computed in a similar manner as for the river system (eq. 12). Evapotranspiration is computed for nodes having ponding depths less than the open-water ponding depth ($H_{i,j,t} < O_{i,j}$) as

$$E_{i,j,t+1} = \left[(Emax_{i,j} - k_{i,j,t+1}) \left(\frac{H_{i,j,t}}{O_{i,j}} \right) + k_{i,j,t+1} \right] e_{i,j}, \quad (36)$$

where k is a daily evapotranspiration coefficient that is interpolated from mid-month values. Both O and k are estimated values that are functions of land-use type and included as part of the input data set.

Evapotranspiration for dry nodes is computed as a function of depth to the ground-water surface. If the depth to ground water is greater than the depth to the deep root zone, $D_{i,j}$ (or $h_{i,j,t} < D_{i,j}$; fig. 6) then $E_o = 0$. If the depth to ground water is greater than the depth to the shallow root zone, $d_{i,j}$, and less than that to the deep root zone (or $D_{i,j} \leq h_{i,j,t} \leq d_{i,j}$; fig. 6), E_o is computed as

$$E_{i,j,t+1} = k_{i,j,t+1} e_{i,j}. \quad (37)$$

$D_{i,j}$ and $d_{i,j}$ are input values and vary with vegetation type. If the depth to ground water is less than the shallow root zone (or $d_{i,j} < h_{i,j,t} < Z_{i,j}$; fig. 6), E_o is

$$E_{i,j,t+1} = k_{i,j,t+1} e_{i,j} \frac{(D_{i,j} - (Z_{i,j} - h_{i,j,t}))}{(D_{i,j} - d_{i,j})}. \quad (38)$$

Finally, the evapotranspiration is subtracted from the ponding depth. If the evapotranspiration exceeds the available water for a node, the excess evapotranspiration is subtracted from the recharge term in the ground-water flow equation. Evapotranspiration is not limited when subtracted from recharge, so it is theoretically possible for recharge to become negative.

Boundary Conditions

Overland flow boundary types are no flow, tidal stage, and a water slope. Boundary location and type are determined by logical statements in the source code of the NSM program and cannot be changed by altering the input data file.

No-flow boundary conditions are used by default at grid boundaries when no boundary conditions are explicitly set by program statements and input data. Boundary water-surface elevations are not explicitly set at most of the northern and western boundaries of the grid. Consequently, at these nodes where boundaries are not specified, initial conditions and the depths calculated at the previous time step are used as the boundary water-surface elevations.

The tidal stage boundary condition is used along the Atlantic coast boundary and is

$$H_{i,j,t+1} = Z_{\text{tide},t+1} - Z_{i,j}, \quad (39)$$

where Z_{tide} is the water-surface elevation due to tide. Tidal stages are computed for each node by using mean monthly tidal stages that were measured at selected boundary nodes. Values for other nodes are then computed by linearly interpolating in space and time from the nodes with measured tidal data.

The water slope boundary condition is used along the southwestern edge of the model grid, at the boundary between the ENP and the Gulf of Mexico (fig. 1). This boundary condition is similar to the commonly used normal depth condition. For solutions proceeding from west to east and north to south (fig. 7A), this boundary is expressed as

$$H_{i,j,t+1} = \frac{1}{2}(H_{i,j-1,t} + H_{i+1,j,t}) \quad (40)$$

when

$$\frac{1}{2}(Z_{i,j-1,t} + Z_{i+1,j,t}) > Z_{i,j,t}.$$

Otherwise, $H_{i,j,t+1} = \delta_{ij}$, where δ_{ij} is the detention depth. If no node exists at $j-1$, $H_{i,j,t+1} = H_{i+1,j,t}$. For the solutions proceeding from east to west, south to north the boundary is expressed as

$$H_{i,j,t+1} = \frac{1}{2}(H_{i,j+1,t} + H_{i+1,j,t}) \quad (41)$$

when

$$\frac{1}{2}(Z_{i,j+1,t} + Z_{i+1,j,t}) > Z_{i,j,t}.$$

Otherwise, $H_{i,j,t+1} = \delta_{ij}$. If no node exists at $j+1$, then $H_{i,j,t+1} = H_{i+1,j,t}$.

Ground-Water Flow

The two-dimensional equation for unconfined ground-water flow is solved to simulate ground-water flow in the NSM. The numerical solution of this equation, along with applied boundary conditions, are presented in this section.

Equations

The ground-water system equation is solved after the overland-flow equations. The two-dimensional equation for unconfined ground-water flow is

$$\frac{\partial}{\partial x} \left(T_{xx} \frac{\partial h}{\partial x} \right) + \frac{\partial}{\partial y} \left(T_{yy} \frac{\partial h}{\partial y} \right) = S \frac{\partial h}{\partial t} + R_{gw}, \quad (42)$$

where

T_{xx} and T_{yy} are the aquifer transmissivities (units of length squared per time),

S is the storage coefficient,

h is the ground-water elevation, and

R_{gw} is the recharge (units of length per time).

Transmissivity is defined as $T = (h + \zeta) \kappa$, where ζ is the aquifer depth measured from a common datum (fig. 6), and κ is the hydraulic conductivity (units of length per time).

Equation 42 is a diffusion-type equation and is solved explicitly at new time steps for h , the ground-water elevation, in the NSM by using a finite-difference formulation which is forward in time and central in space. This technique is an asymmetric numerical approximation that was introduced by

Saul'yev (Ames, 1992) and is described in standard numerical texts (Lapidus and Pinder, 1982). Both forms of the asymmetric numerical approximation (Saul'yev I and Saul'yev II) are used in the NSM code. When the solution proceeds from west to east and south to north (fig. 8A), the form of the equation used to determine the ground-water elevations is

$$\begin{aligned}
h_{i,j,t+1} = & \left[(\kappa_{i+1,j}(\zeta_{i+1,j} + h_{i+1,j,t}) + \kappa_{i,j}(\zeta_{i,j} + h_{i,j,t})) \frac{(h_{i+1,j,t} - h_{i,j,t})}{2\Delta x^2} \right. \\
& + (\kappa_{i,j}(\zeta_{i,j+1} + h_{i,j+1,t}) + \kappa_{i-1,j}(\zeta_{i-1,j} + h_{i-1,j,t+1})) \frac{h_{i-1,j,t+1}}{2\Delta x^2} \\
& + (\kappa_{i,j+1}(\zeta_{i,j+1} + h_{i,j+1,t}) + \kappa_{i,j}(\zeta_{i,j} + h_{i,j,t})) \frac{(h_{i,j+1,t} - h_{i,j,t})}{2\Delta y^2} \\
& + (\kappa_{i,j}(\zeta_{i,j} + h_{i,j,t}) + \kappa_{i,j-1}(\zeta_{i,j-1} + h_{i,j-1,t+1})) \frac{h_{i,j-1,t+1}}{2\Delta y^2} + S_{i,j} \frac{h_{i,j,t}}{\Delta t} - R_{i,j,t+1} \left. \right] \\
& \div \left[\frac{S_{i,j}}{\Delta t} + (\kappa_{i,j}(\zeta_{i,j} + h_{i,j,t}) + \kappa_{i-1,j}(\zeta_{i-1,j} + h_{i-1,j,t+1})) \frac{1}{2\Delta x^2} \right. \\
& \left. + (\kappa_{i,j}(\zeta_{i,j} + h_{i,j,t}) + \kappa_{i,j-1}(\zeta_{i,j-1} + h_{i,j-1,t+1})) \frac{1}{2\Delta y^2} \right].
\end{aligned} \tag{43}$$

For solutions proceeding from east to west and north to south (fig. 8B), the equation is

$$\begin{aligned}
h_{i,j,t+1} = & \left[(\kappa_{i+1,j}(\zeta_{i+1,j} + h_{i+1,j,t+1}) + \kappa_{i,j}(\zeta_{i,j} + h_{i,j,t})) \frac{h_{i+1,j,t+1}}{2\Delta x^2} \right. \\
& - (\kappa_{i,j}(\zeta_{i,j} + h_{i,j,t}) + \kappa_{i-1,j}(\zeta_{i-1,j} + h_{i-1,j,t})) \frac{(h_{i,j,t} - h_{i-1,j,t})}{2\Delta x^2} \\
& + (\kappa_{i,j+1}(\zeta_{i,j+1} + h_{i,j+1,t+1}) + \kappa_{i,j}(\zeta_{i,j} + h_{i,j,t})) \frac{h_{i,j+1,t+1}}{2\Delta y^2} \\
& - (\kappa_{i,j}(\zeta_{i,j} + h_{i,j,t}) + \kappa_{i,j-1}(\zeta_{i,j-1} + h_{i,j-1,t})) \frac{(h_{i,j,t} - h_{i,j-1,t})}{2\Delta y^2} + S_{i,j} \frac{h_{i,j,t}}{\Delta t} - R_{i,j,t+1} \left. \right] \\
& \div \left[\frac{S_{i,j}}{\Delta t} + (\kappa_{i+1,j}(\zeta_{i+1,j} + h_{i+1,j,t+1}) + \kappa_{i,j}(\zeta_{i,j} + h_{i,j,t})) \frac{1}{2\Delta x^2} \right. \\
& \left. + (\kappa_{i,j+1}(\zeta_{i,j+1} + h_{i,j+1,t+1}) + \kappa_{i,j}(\zeta_{i,j} + h_{i,j,t})) \frac{1}{2\Delta y^2} \right].
\end{aligned} \tag{44}$$

Information from five nodes is used in calculating h at the new time step (fig. 8). Information at two of the nodes used in equations 43 and 44 is at the new time step, $t+1$. The rest of the information is for the previous time step, t .

If the ground-water elevation at $t+1$ is greater than the land-surface elevation, the ponding depth is updated to be

$$H_{i,j,t+1} = H_{i,j,t+1} + (h_{i,j,t+1} - Z_{i,j})S_{i,j}. \tag{45}$$

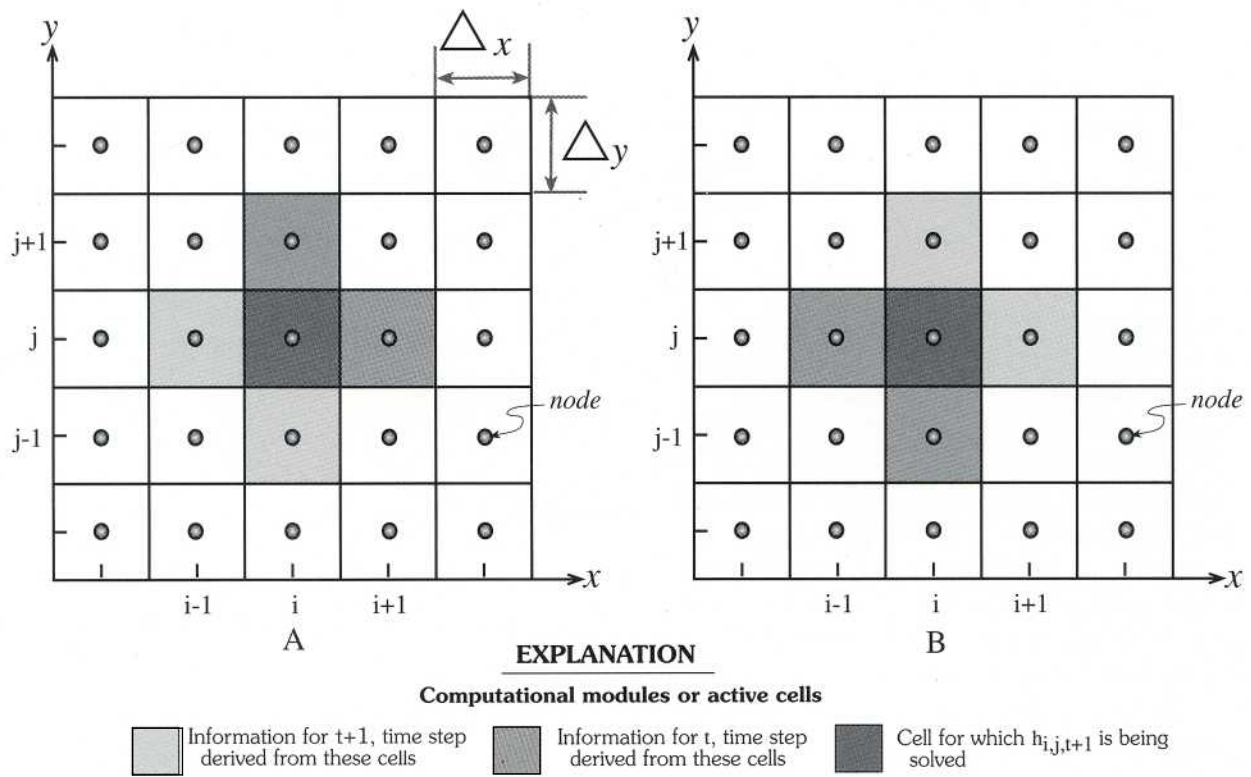


Figure 8. Computational modules or active cells in a grid fragment for the ground-water computations for $h_{i,j,t+1}$ proceeding from (A) west to east and south to north, and (B) east to west and north to south.

The computed ground-water elevation, $h_{i,j,t+1}$, is then reset so that $h_{i,j,t+1} = Z_{i,j}$. Hence, the ground-water elevation cannot exceed the land-surface elevation.

The recharge term, R_{gw} , includes the flow between the river and ground-water systems, R_r , and the infiltration or seepage from the overland-flow system, I , so that

$$R_{gw(i,j,t+1)} = R_{r(i,t+1)} + I_{i,j,t+1}. \quad (46)$$

Boundary Conditions

Ground-water flow boundaries are defined by either tidal stage, or as a no-flow boundary. Boundary locations and type are determined by logical statements in the source code of the NSM program. Boundary locations and type cannot be changed by altering the input data file.

The tidal-stage boundary conditions are applied along the Atlantic coast. At these boundary nodes,

ground-water level is set to equal the tidal water-surface elevation, or stage. Tidal stages are computed for each node by using mean monthly tidal stages that were measured at selected boundary nodes. Values for other nodes are then computed by linearly interpolating in space and time from the nodes with measured tidal data.

The no-flow boundary condition is used at all boundaries other than the tidal boundary. The no-flow condition is created by setting ground-water elevations across the boundary (within the model domain, and just outside the domain) to the same elevation so that there is no water-surface gradient. When the computational module spans the boundary so that a known node (or nodes) is outside the model domain, equations 43 and 44 are solved in the NSM by using information for the center node at the previous time step for the node outside the grid. However, direct substitution of the center node information from the previous time step into equations 43 and 44 for the nodes outside the domain does not necessarily ensure a no-flow condition.

Substitution of the information from the center node at the previous time step, t , for the node at the $i,j+1,t+1$ location along the southern boundary results in an extra term in equation 43 applied at the southern boundary. Similarly, substitution of the information from the center node at the previous time step, t , for node $i-1,j,t+1$ results in an extra term in equation 43 applied at the western boundary. Consequently, when equation 43 is used to describe ground-water levels at the southern and western boundaries, the no-flow boundary condition is not guaranteed because of these extra terms. In the same manner, application of equation 44 does not guarantee no flow at the eastern and northern boundaries because of the error.

The forms of the equations (eqs. 43 and 44) used to solve for $h_{i,j,t+1}$ result from rearranging terms of the governing equations in order to solve for the unknown. But, more primitive forms of the equations 43 and 44 are needed to ensure that the no-flow condition is properly applied. The appropriate no-flow boundary condition for the computational module in figure 8A for the southern boundaries is

$$h_{i,j,t+1} = \left[(w_{i+1,j,t} + w_{i,j,t}) \frac{(h_{i+1,j,t} - h_{i,j,t})}{2\Delta x^2} \right. \quad (47)$$

$$+ (w_{i,j,t} + w_{i-1,j,t+1}) \frac{h_{i-1,j,t+1}}{2\Delta x^2}$$

$$+ (w_{i,j,t} + w_{i,j+1,t}) \frac{(h_{i,j+1,t+1} - h_{i,j,t})}{2\Delta y^2}$$

$$\left. + S_{i,j} \frac{h_{i,j,t}}{\Delta t} - R_{i,j} \right] \div \left[\frac{S_{i,j}}{\Delta t} + \frac{(w_{i,j,t} + w_{i-1,j,t+1})}{2\Delta x^2} \right],$$

where $w_{i,j,t} = \kappa_{i,j}(\zeta_{i,j} + h_{i,j,t})$. Likewise the no-flow boundary condition for the western boundaries should be

$$h_{i,j,t+1} = \left[(w_{i+1,j,t} + w_{i,j,t}) \frac{(h_{i+1,j,t} - h_{i,j,t})}{2\Delta x^2} \right. \quad (48)$$

$$+ (w_{i,j+1,t} + w_{i,j,t}) \frac{(h_{i,j+1,t} - h_{i,j,t})}{2\Delta y^2}$$

$$+ (w_{i,j,t} + w_{i,j-1,t+1}) \frac{h_{i,j-1,t+1}}{2\Delta y^2}$$

$$\left. + S_{i,j} \frac{h_{i,j,t}}{\Delta t} - R_{i,j} \right] \div \left[\frac{S_{i,j}}{\Delta t} + \frac{(w_{i,j,t} + w_{i,j-1,t+1})}{2\Delta y^2} \right].$$

For the computational module in figure 8B, the northern boundary conditions should be computed as

$$h_{i,j,t+1} = \left[(w_{i+1,j,t+1} + w_{i,j,t}) \frac{h_{i+1,j,t+1}}{2\Delta x^2} \right. \quad (49)$$

$$- (w_{i,j,t} + w_{i-1,j,t}) \frac{(h_{i,j,t} - h_{i-1,j,t})}{2\Delta x^2}$$

$$- (w_{i,j,t} + w_{i,j-1,t}) \frac{(h_{i,j,t} - h_{i,j-1,t})}{2\Delta y^2}$$

$$\left. + S_{i,j} \frac{h_{i,j,t}}{\Delta t} - R_{i,j} \right] \div \left[\frac{S_{i,j}}{\Delta t} + \frac{(w_{i+1,j,t+1} + w_{i,j,t})}{2\Delta x^2} \right],$$

and the eastern boundaries should be computed as

$$h_{i,j,t+1} = \left[(w_{i,j+1,t+1} + w_{i,j,t}) \frac{h_{i,j+1,t+1}}{2\Delta y^2} \right. \quad (50)$$

$$- (w_{i,j,t} + w_{i-1,j,t}) \frac{(h_{i,j,t} - h_{i-1,j,t})}{2\Delta x^2}$$

$$- (w_{i,j,t} + w_{i,j-1,t}) \frac{(h_{i,j,t} - h_{i,j-1,t})}{2\Delta y^2}$$

$$\left. + S_{i,j} \frac{h_{i,j,t}}{\Delta t} - R_{i,j} \right] \div \left[\frac{S_{i,j}}{\Delta t} + \frac{(w_{i,j+1,t+1} + w_{i,j,t})}{2\Delta y^2} \right].$$

REVIEW OF SELECTED FEATURES OF THE NATURAL SYSTEM MODEL

Complete technical details of the review of the NSM are documented in three technical memoranda from the USGS to the U.S. Army Corps of Engineers. In this section, results from the review are briefly summarized, information from the memoranda is updated, where appropriate, and NSM simulations are compared with simulations from another two-dimensional numerical model. Conclusions—including findings presented in the section, “Governing Equations and Boundary Conditions”—also are summarized in this section.

The review was performed using NSM version 4.3. With the exception of a few cases, simulations were performed for a period of 1 year by using the 1965 input data provided by the SFWMD.

As the review progressed and findings were released, SFWMD staff addressed many of the issues

by revising NSM version 4.3 and releasing version 4.4. A brief summary of these changes and the effects of the NSM revisions on simulation results also are presented in this section.

Initial and Boundary Conditions

Initial conditions and model boundary data for 1965 were briefly reviewed for consistency and reasonableness. The development of automated routines to perform range checking on input data sets and boundary data would help to ensure that incorrect values were not included in these data files. Automated routines are needed because of the large size of the data sets.

Unusually high water levels were observed in the Atlantic coast boundary at the beginning of calendar year 1965. Some of the water levels were as high as 14 ft mean sea level along the southeast boundary. These high water levels had subsided by June 1965, and the effect of this inconsistent initial condition likely was not present in simulated results after 1966. These high water levels were attributed to an initial condition which established a uniform ponding depth over the entire model domain of 1 ft, regardless of land-surface elevation.

Input data included ground-water storage coefficients greater than one. These storage coefficients resulted in the simulation of negative ponding depths for some simulations. Changes are easily made to the storage coefficient input data.

Monthly mean tidal boundaries are not consistent with the climatic inputs to the model, which are at a daily time step. It would be more consistent to use 1965–90 daily mean tidal elevations as the tidal boundaries. Other reasonable alternatives might include daily maximum and minimum tidal elevations, or the use of tidal harmonics derived from 1965–90 data to generate tidal boundaries. It is not likely, however, that this change in the tidal boundaries would affect simulated water levels and hydroperiods, except perhaps at the extreme southern end of the model domain.

The no-flow ground-water boundaries are not always ensured using the formulations in NSM version 4.3. Equations 47–50 will ensure the no-flow condition. The absence of consistent no-flow ground-water boundaries probably has minimal effect on simulated water levels and hydroperiods.

The effect of changes in initial conditions on simulation results was evaluated by reducing Lake Okeechobee and Lake Hicpochee initial water levels by 1 ft from the levels used in NSM version 4.3. Simulation results from the NSM 4.3 were compared with those made by using the lower initial lake water levels. Mean water levels in the model domain for the two sets of initial conditions differed by about 0.4 ft after 1 year of simulation. This indicates that the effects of changes in initial conditions remain in the model for a minimum of more than 1 year, and that at least the first 2 years of simulation results should be omitted from the analysis of results. An alternative, and perhaps preferred, scenario for eliminating the effects of initial conditions on simulation results is to apply the model with 1965–90 mean boundary conditions as the first 2 or more years of input data. Further analysis of the effects of changes in initial conditions on simulated results is warranted.

Computational Grid Size and Time Step

The NSM solves equations that are fundamentally continuous in time and space on a finite-difference computational grid (1) consisting of square computational cells that are 2 mi long on a side and (2) using a daily or 6-hour computational time step. The continuous governing equations are assumed to be adequately approximated by the discontinuous (or finite-difference) space and time steps used to obtain a solution. The size of the computational cells and time step relate directly to the manner in which the physical processes are represented in the model and to the solution obtained. If the appropriate combination of time and spatial finite-differences is used in the NSM, then any additional decrease in the size of the space or time step will result in no appreciable change in model results, and the model is said to be convergent (Roache, 1982; Thompson, 1992). The effects of smaller time steps (less than daily) and computational cells (less than 2 mi by 2 mi) on NSM results were evaluated.

A computational grid consisting of square cells which were 2/3-mi long on a side was produced using the data from the original grid. There was no change in the resolution of the vegetation, topographic, or land-use information; the only change was in the number of cells used to represent the system. Nine computational cells in the 2/3-mi grid replaced one computational cell in the 2-mi grid, but the location of the solution point (node) in each of the 2-mi cells coincided with the

location of a solution point (node) in one of the 2/3-mi cells.

Simulations also were made with the 2-mi cells and time steps of 8, 6, 3, 0.5, and 0.05 hours. All processes (river, overland, and ground water) were simulated at the time step. Daily precipitation was distributed uniformly throughout the day. For example, for the 8-hour time step, one-third of the daily precipitation was added to each cell at the beginning of each 8-hour interval. Results from simulations made using different temporal and spatial resolution, but with the same grid velocity (ratio of grid size to computational time step) were compared. All simulation results presented in this section were made using 1965 input data.

Simulated mean ponding depth and depth to ground water were generally insensitive to temporal and spatial resolution (table 2). For a grid velocity of 0.12 ft/s (fig. 9), the maximum difference in the simulated mean ponding depths for the two sets of time-space steps was about 0.3 ft, and the maximum difference in the mean depth to ground water was about 0.04 ft. The maximum difference in mean ponding depths was about 0.4 ft for the two sets of time-space steps having a grid velocity of about 0.35 ft/s (fig. 10), and the maximum difference in mean depth to ground water was about 0.03 ft. Increased resolution resulted in smaller simulated ponding depths and little change in depths to ground water for both sets of grid velocities.

Table 2. Mean ponding depths and depths to ground water as a function of computational grid size and time step

[mi, miles; ft/s, feet per second; ft, feet]

Time step (hours)	Grid size (mi)	Grid velocity (ft/s)	Mean ponding depth (ft)		Mean depth to ground water (ft)	
			Maximum (Oct.)	Minimum (May)	Maximum (May)	Minimum (Oct.)
24	2	0.12	1.98	0.95	1.89	0.17
8	2/3	.12	1.70	.74	1.90	.14
8	2	.37	1.94	.94	1.87	.14
3	2/3	.33	1.58	.71	1.90	.13

A change in the computational grid size for a constant time step has a greater effect on simulated maximum ponding depths than a change in the time step for a constant grid size (table 2). The effects of

changes in grid size and time step appear to be about the same on simulated maximum depth to ground water.

Water-level differences, ponding depth, and depths to ground water simulated with a range of grid sizes and time steps were compared to values simulated by using NSM version 4.3 with the 2-mi by 2-mi computational cells and a 6-hour time step. Differences between the NSM 4.3 results and simulations made with other combinations of grid size and time step were determined for each cell in the model domain, and the mean and standard deviation of these differences were calculated (table 3).

Changes in the time step had little effect on monthly mean ponding depth for the 2-mi grid (October results shown in table 3). Likewise, water-level differences, ponding depth, and mean depth to ground water simulated with the 2/3-mi grid were relatively unaffected by a change in time step from 8 to 3 hours. However, the difference between monthly mean ponding depths for the 2/3-mi grid and the two time steps was greater than any differences noted between time steps for the 2-mi grid.

Changes in computational grid size had a greater effect on simulated ponding depths than changes in the size of the time step (tables 2 and 3). For the same time-step size, the change in grid size reduced October mean ponding depth from 0.24 ft (8-hour time step) to 0.35 ft (3-hour time step). However, depth to ground water was unaffected by changes in grid size. Results for other months were similar to those for October.

Hydroperiods, defined in this case as the amount (or percent) of time during a year that a specified area is inundated, simulated by using different time steps and 2-mi grid were compared for 1965 input conditions. Hydroperiod changed only slightly as the time-step size was increased. The area of the model domain which was simulated as being dry changed less than 2 percent with all changes in grid size and time step.

The historic water level, ponding depth, depth to ground water, and hydroperiod are unknown. However, these results indicate that simulated ponding depths are somewhat dependent on the magnitude of the grid size. Moreover, the magnitude of the standard deviations of the differences between NSM version 4.3 results and results obtained with the 2/3-mi grid is on the order of the maximum ponding depths in much of the model domain. However, simulated mean depth to ground water and hydroperiod appear to be unaffected by changes in grid size and time step.

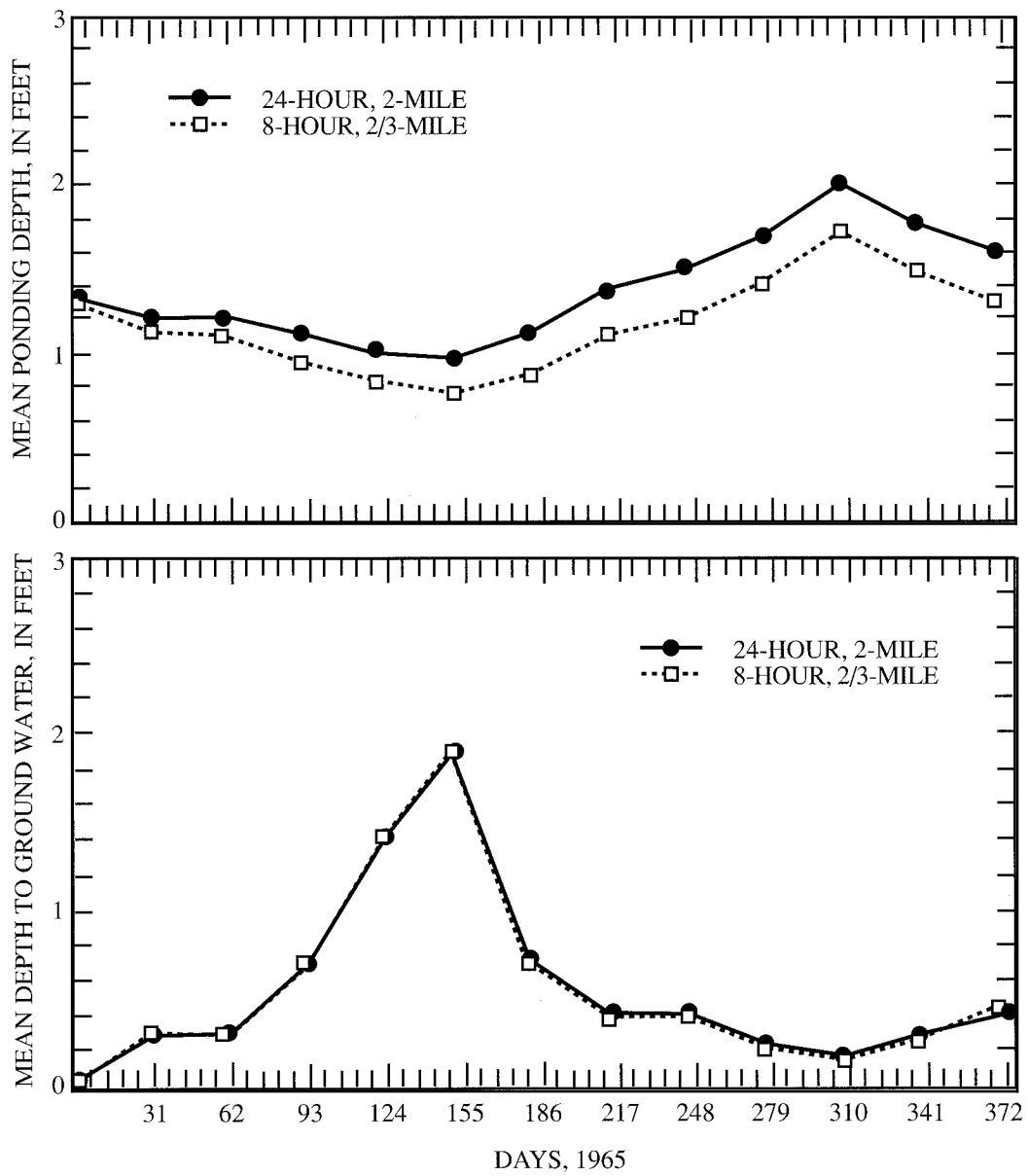


Figure 9. Combined effects of computational cell size and time step on mean ponding depth and mean depth to ground water for a grid velocity of 0.12 foot per second.

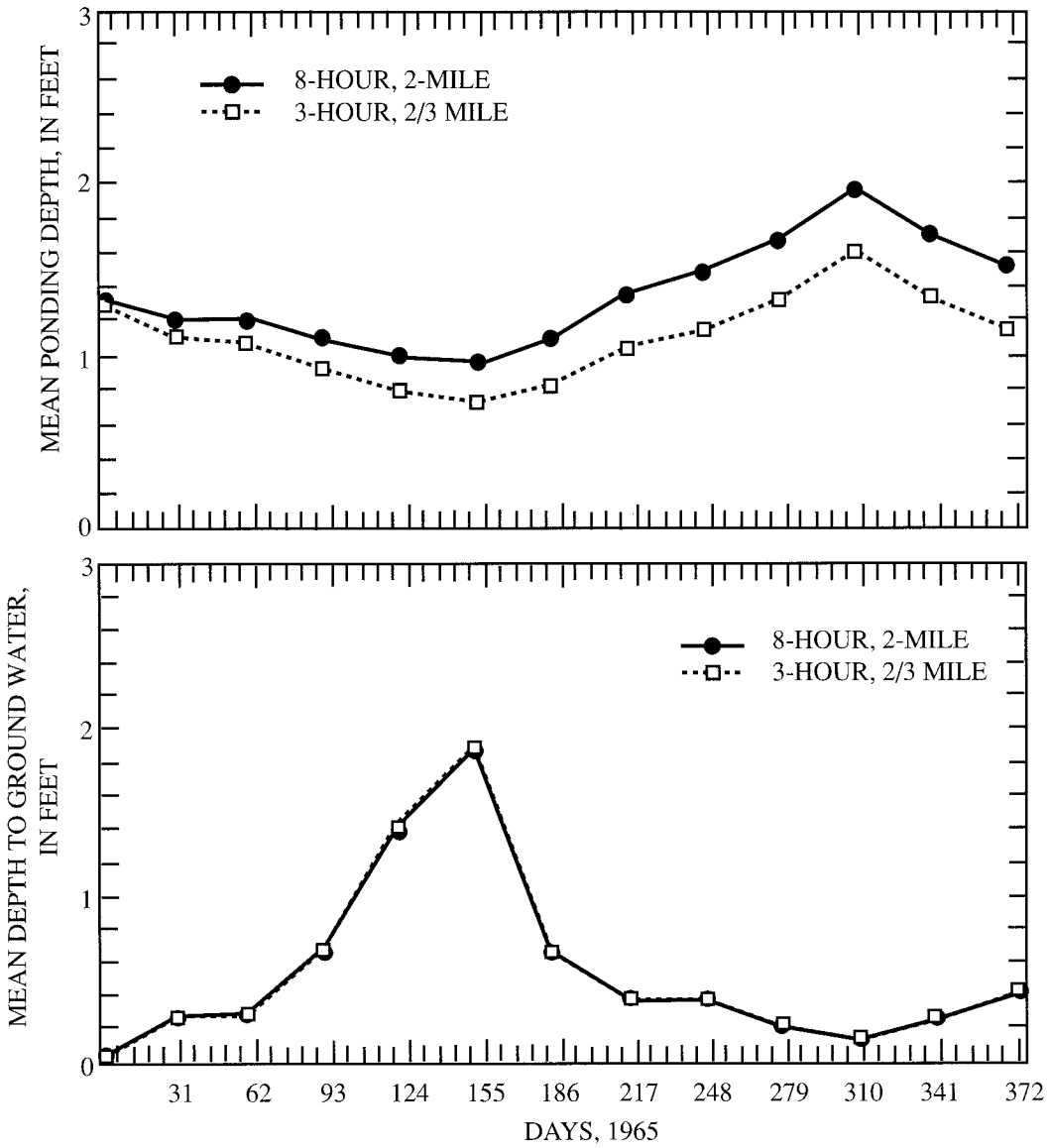


Figure 10. Combined effects of computational cell size and time step on mean ponding depth and mean depth to ground water for a grid velocity of about 0.35 foot per second.

Table 3. Simulated water-level differences, ponding depths, and depths to ground water made by using NSM version 4.3 (2-mile grid, 6-hour time step) and other combinations of grid size and time step for October 1965 conditions

[ft, feet; —, not applicable]

Time step (hours)	Grid size (miles)	Water-level difference (ft)		Ponding depth (ft)		Depth to ground water (ft)	
		Mean	Standard deviation	Mean	Standard deviation	Mean	Standard deviation
24	2	0.17	0.29	1.98	3.68	0.17	2.30
8	2	.02	.04	1.94	3.61	.14	2.15
6	2	—	—	1.94	3.60	.14	2.14
3	2	.04	.07	1.93	3.57	.14	2.14
0.5	2	.06	.10	1.92	3.55	.14	2.14
0.05	2	.09	.14	1.89	3.50	.14	2.15
8	2/3	.74	1.46	1.70	2.82	.14	2.21
3	2/3	.72	1.56	1.58	2.67	.13	2.20

As previously indicated, a model is considered to be convergent if a decrease in the size of the time or space step results in no appreciable change in model results. The fact that simulated ponding depths are a function of grid size does not necessarily mean that the model algorithms are incorrect or that an inappropriate numerical scheme has been used to solve the equations. Rather, the size of the spatial finite difference used to discretize the continuous differential equations probably has not been chosen appropriately for the particular problem. Consequently, the simulations appear to remain a function of the magnitude of the grid size.

River System

Rivers in the NSM are treated as reservoirs. The upstream inflow is defined in the input data set, ground-water seepage is computed using a Darcy relation (eq. 10), exchange between the river and the overland-flow system is simulated using the Manning equation (eq. 5), and outflows from the river system are determined using a weir equation (eq. 11). The water level in the river is then determined from a mass balance of these flows, precipitation, evapotranspiration, and the volume of water remaining in the river channel (eq. 3).

The primary NSM output of interest to scientists and managers is simulated hydrologic characteristics

of the overland-flow system. The rivers interact with the overland-flow system in two distinct ways—directly through exchange of water between the rivers and overland-flow system, and indirectly through exchange between rivers and the ground-water system, which in turn affects conditions in the overland-flow system.

Three tests were designed to evaluate the sensitivity of NSM results to reasonable changes in the algorithms used to represent rivers in the NSM. First, the weir equation used to compute river outflows was replaced by the Manning equation. A Manning n -value of 0.025 was assumed, and water-surface slope was computed as the difference between the stage in the upstream-most node of the river and the original weir-crest elevation. Consequently, results from this test are still somewhat dependent on the weir assumption. However, the assumption about the downstream water-level boundary was required in the absence of data, and in fact, both algorithms (weir and Manning) are simplifications of a complex system. In the second test, the connection between the river system and the ground-water system was removed to evaluate the effects of the seepage component on river flow. Finally, the connection between the river system and the overland-flow system was removed to evaluate the role of the river system in the overland-flow-dominated NSM.

In order to test the sensitivity of the river-system algorithms to reasonable changes, simulations made

with the original (unmodified) NSM were compared with those made by using the three modifications to the river-system equations for 1965 input and boundary conditions. A root-mean-square (RMS) difference between wetland water levels computed by using the original and the modified algorithms was determined for each test. The RMS difference was computed as the sum of the square of the differences in water levels for the original and modified algorithms for all the cells and all time steps; this sum was then averaged over the model domain, and the square root of the resulting mean value was determined and reported, yielding a single number for each comparison.

The change from the weir assumption to the Manning formulation for representing river outflows had widely varying effects on the different river systems (fig. 11). Both the Manning formulation and the weir assumption are reasonable approaches for representing river flows. River stages simulated by using 1965 input and boundary data for the Miami River and the Boca River (fig. 3) were generally unaffected by the change in the river outflow algorithm. The algorithm change, however, resulted in differences in simulated stage of as much as 3 ft for the Jupiter and New Rivers, and as much as 7 ft for New River Sound (fig. 11). Because the New River Sound is on the coast adjacent to a boundary (fig. 3), simulated water levels in the sound likely do not significantly affect water levels in the overland-flow system. The change in the river outflow algorithm had an insignificant effect on water levels across the entire overland-flow system (table 4), as measured by the RMS value. The sensitivity of overland-flow-system water levels near the Jupiter and New Rivers to changes in river stages may need further analysis.

Removing the connection between the ground-water system and the river system had little effect on simulated stages in the rivers. The largest difference was for the Jupiter River (fig. 12), with a mean-square difference between the two sets of values of only 0.065 ft. Likewise, the RMS difference in overland-flow-system water levels simulated using the two algorithms was 0.046 ft.

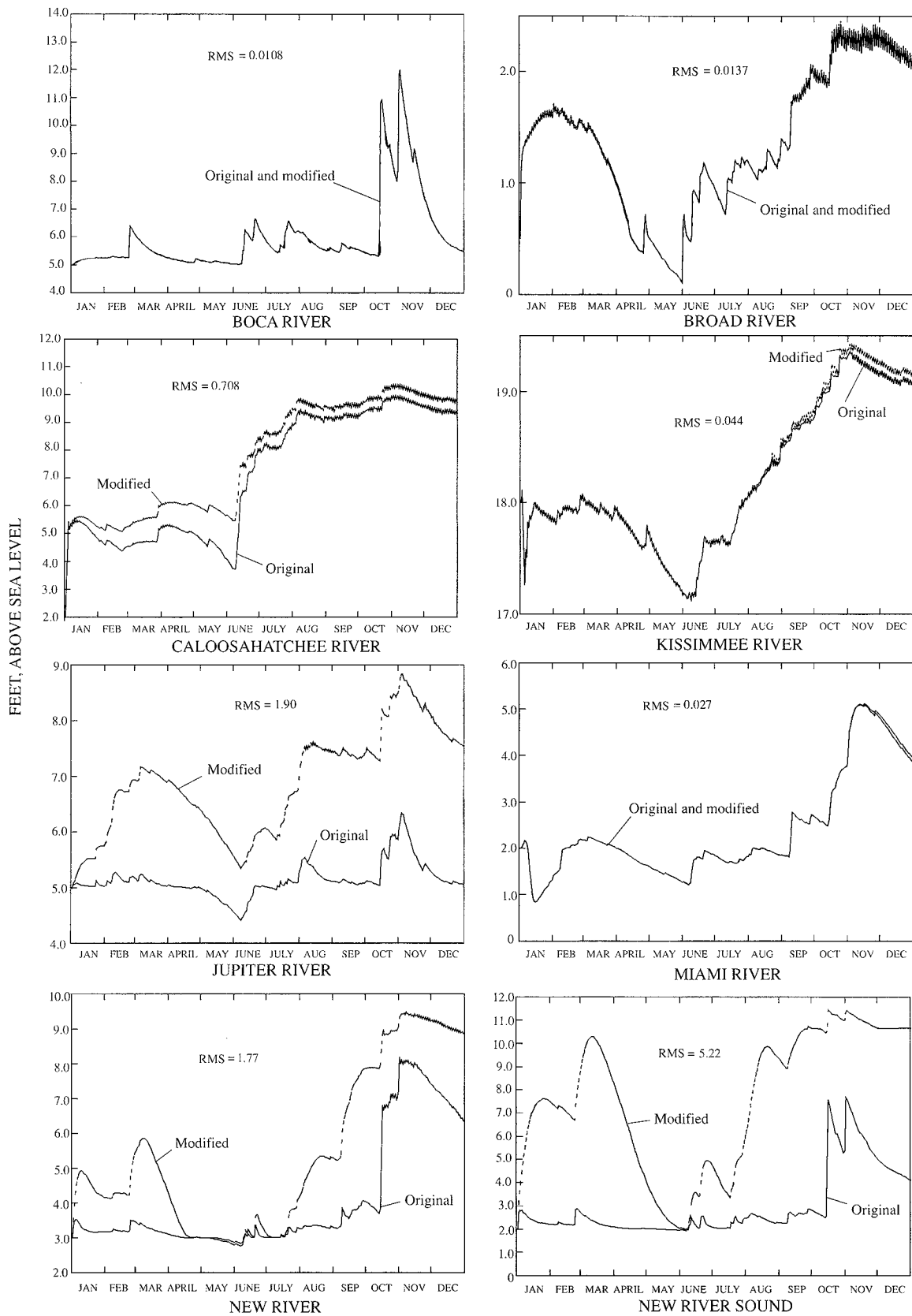
Decoupling the overland and river systems resulted in changes in simulated river stages for some of the rivers (fig. 13). The mean-square differences between river stages simulated by using the two algorithms were similar to those obtained by using the two different river outflow algorithms (fig. 11; table 4).

The largest differences were for the Caloosahatchee and Kissimmee Rivers, both inland systems. The tests indicated that flows in these rivers, as well as in the Boca and Broad Rivers, consist primarily of contributions from the overland-flow system. This is particularly true for the Caloosahatchee River, in which almost all of the flow appears to be from the overland system. Moreover, it appears that the overland system almost always contributes flow to the river system, but the river system seldom contributes flow to the overland system, with the exception of the Kissimmee River in early 1969. As long as the river does not contribute flow to the overland system, then the previously identified absence of a limitation on flow from the river to the overland system does not affect simulation results.

The RMS difference between overland-flow-system stages simulated with and without the overland-river-system coupling was the largest of the three tests (table 4), but still small relative to annual water-level fluctuations. However, it is likely, as with the change in the river outflow algorithm, that locally large

Table 4. Summary of tests of river-system algorithms [ft. feet]

Test	Difference between original and modified algorithms		
	Maximum difference in river stage (ft)	Minimum difference in river stage (ft)	Root-mean-square difference in overland-flow system stage (ft)
River outflows represented by Manning's equation	5.22	0.0108	0.068
No connection between river and ground-water system	.0652	.0006	.046
No connection between river and overland-flow system	5.58	.20	.076



1965

Figure 11. Stages computed for eight NSM rivers by using the original NSM river outflow algorithm and a modified algorithm based on the Manning equation.

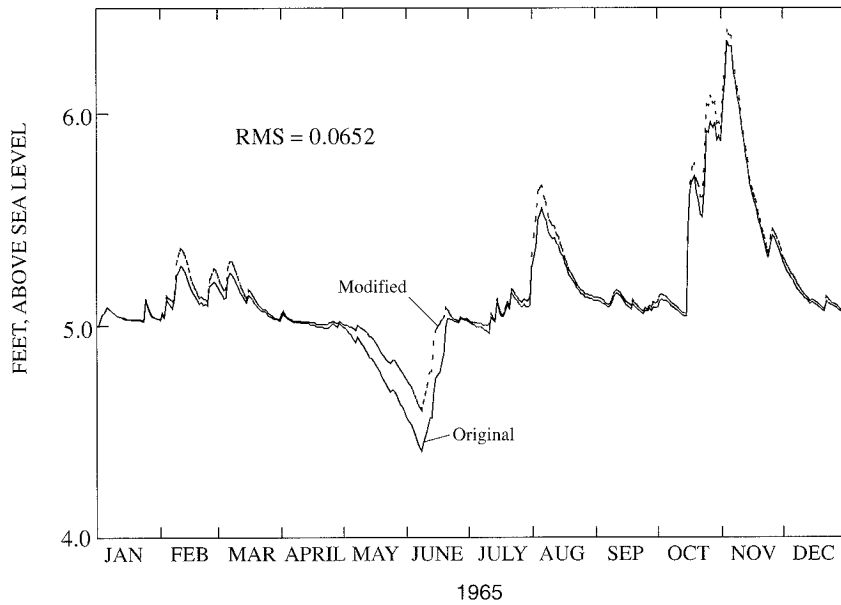


Figure 12. Jupiter River stage computed by using the original NSM river-system algorithm and a modified river-system algorithm in which there is no coupling between the river and ground-water systems.

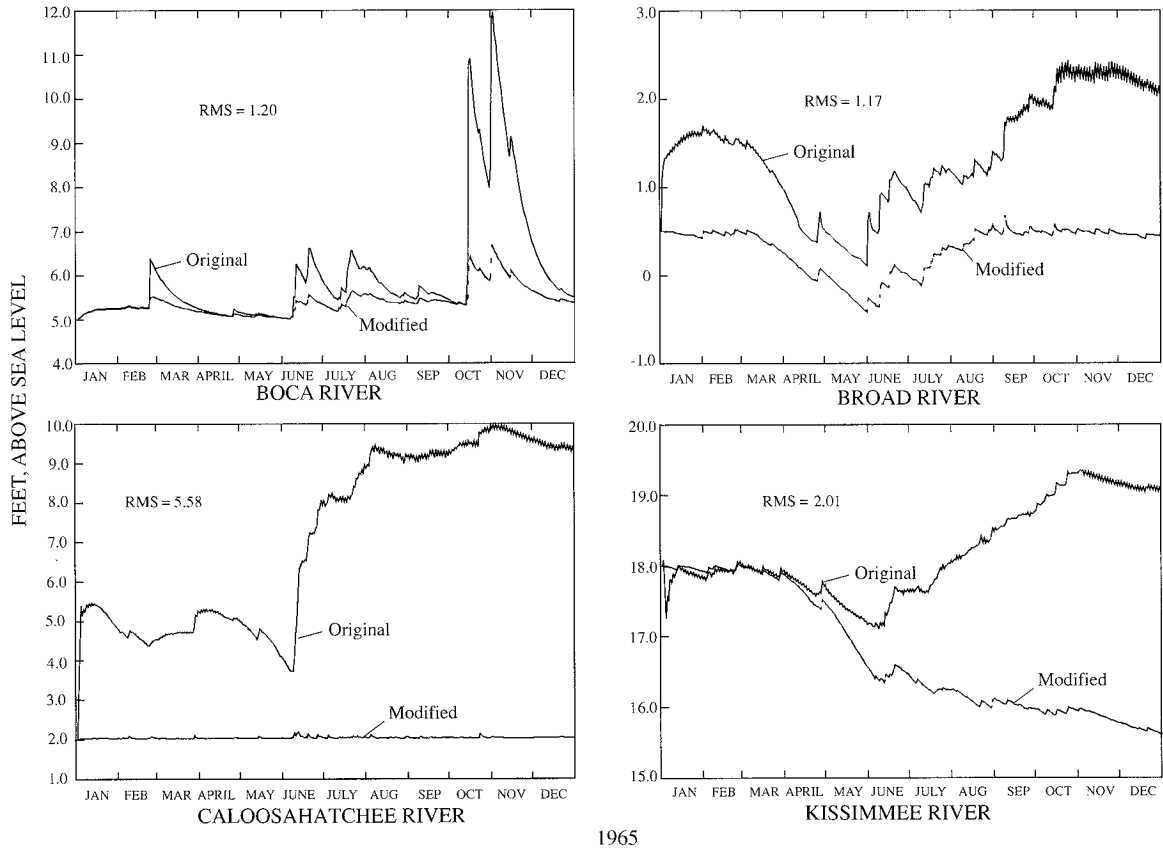


Figure 13. Stages computed for four NSM river systems by using the original NSM river-system algorithm and a modified algorithm in which there is no coupling between the overland-flow and river systems.

differences in overland-flow-system stages exist when the two different algorithms are used. Results of these tests also indicate that the coupling of the river and the overland-flow systems is the most important component of the river-system simulations.

Oscillations in river stage were present for most of the rivers (fig. 11); the maximum amplitude was about 0.2 ft. Oscillations are not evident when the river and overland-flow systems are decoupled (fig. 13). This may be because river stages are much lower and oscillations do not appear to occur at lower stages. More likely, however, the oscillations in river stage result from the solution of the overland-flow-system equations and are transferred to the river system when the two systems are coupled. When the systems are decoupled, the oscillations in the simulated overland-flow-system stages are not passed to the river system. Evidence of this exists in Kissimmee River stages for the first 4 to 5 months of 1965, when river stages simulated with the two algorithms were almost the same, but oscillations were present only in stages simulated with the coupled overland-flow/river-system algorithm (fig. 13).

It is likely that the oscillations are a result of application of the flux limiter (eq. 34) in the solution of the overland-flow equations. The flow routine attempts to move water through more than one cell during a single time step, but the flux limiter prevents this and levels the water surface between adjacent cells. Then, during the next time step, little or no flow occurs because of the low water-surface gradient. When additional inflow occurs from rainfall or upstream flow, the water-level gradient again increases, and flow increases again until the flux limiter is applied.

Overland-Flow System

Evapotranspiration in the NSM is computed by using a modified Penman-Monteith technique. Evapotranspiration for individual cells is determined by using an inverse-distance weighting scheme. Pan evaporation data are used to determine evaporation from Lake Okeechobee. In general, evapotranspiration is computed as the product of the pan evaporation and a crop coefficient, which is a function of vegetation type, month, and water level.

The crop coefficient used in the NSM varies seasonally and with vegetation type. However, the 3 months which generally have the highest crop coefficient are February, March, and April, and the

3 months with the lowest coefficient are January, December, and June. In fact, the NSM crop coefficients, which are determined as part of the SFWMM calibration, have a bi-modal distribution, with local minima in June, December, and January, and local maxima in March and September.

Computer code was prepared to write the maximum and minimum simulated overland-flow velocity in the model domain during each time step to a file. The maximum overland-flow velocity simulated with NSM version 4.3 for 1965 was 11 ft/s for the 2-mi grid and 6-hour time step. This velocity, which occurred north of Lake Okeechobee, is unreasonably high and indicates input data errors or weaknesses in the model algorithms. Unusually high velocities occurred throughout the model domain during simulations, although computer code was not written to quantify the statistics of the velocity distributions in each computational cell for the year-long simulation. Because of the way in which the overland-flow equations are solved, by using information from adjacent cells and previous time steps to compute velocities in the unknown cell (fig. 7), the effects of these high velocities will be propagated through the model domain for the present and subsequent time steps.

In a typical application of NSM version 4.3, velocities are generally reviewed on a time-averaged basis to examine seasonal, annual, or multi-year flow patterns. Simulated velocities could be checked and other potential problems identified if annual maximum, minimum, and mean velocities for each computational cell were written to a file for subsequent checking and analysis.

Tests indicated that the volume limiter was applied almost 15 million times for 1 year of simulations with the 2-mi grid and a 30-minute time step. This means that the limiting function was applied to about 37 percent of the computations during the 1-year simulation.

NSM version 4.3 was modified by USGS staff in order to perform selected tests for this study. These modifications include (1) addition of a check to ensure that outflow from the river system to the overland-flow system does not exceed the available river flow volume, (2) correction of the ground-water no-flow boundary conditions (eqs. 47–50), and (3) modification of the overland-flow routines to include a length-weighted roughness value. The maximum simulated velocity for 1965 obtained with this modified program was 1.5 ft/s,

which is more reasonable than 11 ft/s, but still probably too high for the south Florida system. These program modifications did not significantly affect the mean ponding depth or mean depth to ground water simulated using 1965 climatic data, but cell-by-cell comparisons were not made. Moreover, effects of these modifications to model algorithms on longer simulations were not identified.

Natural System Model Version 4.3 and Two-Dimensional Hydrodynamic Model Overland-Flow Simulations

Overland flows and ponding depths simulated by using the NSM were compared with overland-flow simulations made with a hydrodynamic model. Comparisons were made because of the importance of overland flow in the natural system and the need to evaluate results from two approaches for solving the overland-flow problem. The two approaches were not entirely independent, however, because a time series of NSM-simulated water levels was used as input to the hydrodynamic model.

The hydrodynamic model TRIM (tidal residual, intertidal mudflat), developed by Cheng and Casulli (1992), was applied to the portion of the NSM domain south of Tamiami Trail. TRIM uses a semi-implicit finite-difference method for solving the complete two-dimensional depth-averaged hydrodynamic equations (Casulli, 1990). TRIM also simulates the flooding and emergence of marshes, shoals, and other similar features. The model solves the continuity, *x*-direction momentum, *y*-direction momentum, and salt transport equations, and an equation of state for the unknown *x*-velocity, *y*-velocity, water depth, salt concentration, and density. Salinity was zero in this application. Land-surface elevation, vegetation, and land use were the same for corresponding TRIM and NSM computational cells.

The evapotranspiration routine in the NSM was incorporated into TRIM by adding a sink term to the continuity equation. The NSM routine uses vegetation-based parameters to compute the evapotranspiration, and the vegetation designation for each cell in TRIM was the same as that used in the NSM. If a computational cell was dry, the evapotranspiration was set equal to zero for that cell in TRIM, which is different from the routine used in the NSM. Rainfall was added to each TRIM computational cell in a manner similar to that done for the NSM. Both the

evapotranspiration and rainfall routines added to TRIM were thoroughly checked to ensure that these processes were accurately represented during the model simulations. Ground-water flow was not included in TRIM. Data for 1965 were used for the simulations.

The TRIM model domain was bounded by the Tamiami Trail to the north, the Atlantic Ocean to the east, and Florida Bay to the south and west. The rectangular finite-difference grid used to represent this domain consisted of 920 computational cells, 2-mi by 2-mi each. Land-surface elevations for TRIM were the same as those in the NSM. A 60-second time-step and an eddy diffusivity coefficient of 2.0 feet squared per second were used. Manning coefficients ranged from 0.028 for water depths less than 1 ft, to 0.016 for depths greater than 10 ft. Boundary conditions were the NSM-simulated stages at Tamiami Trail and the NSM tidal boundaries in Florida Bay and the Atlantic Ocean. Greater agreement between TRIM and the NSM might be expected near the northern boundary of the TRIM model domain because NSM results were used as input to TRIM. Consequently, comparison of the simulations by the two models was limited to the lower 75 percent of the model domain.

The NSM-simulated water levels and flow rates in each computational cell (excluding the northern-most 25 percent of the grid) were statistically compared to those simulated by TRIM. There were rather significant differences between the two sets of results in a few isolated locations, which were primarily in the cells that became dry during the dry season. The absolute value of the maximum difference in simulated water levels was 31 percent, and the absolute value of the maximum difference in simulated flow rates was 26 percent (table 5). Overall, however, results from the two models agreed reasonably well. The average percent absolute difference for all three dependent variables was less than 10 percent.

Table 5. Comparison of NSM and TRIM results

Simulated variable	Absolute value of difference between NSM and TRIM results (percent)		
	Maximum	Minimum	Average
Water level	31	1	7
North-south flow	26	4	9
East-west flow	19	3	7

Minor differences were noted in the simulated directions of flow by the two models, with the largest difference in and near Taylor Slough. The fairly coarse grid used in both models, which yielded an equally coarse predicted flow pattern, coupled with the differences in the wetting and drying routines used in the two models, diminishes the significance of the noted minor differences in the simulated flow directions.

Natural System Model Version 4.4

Changes made to NSM version 4.3, which resulted in version 4.4, are briefly documented in this section. Changes were made by SFWMD staff, primarily in response to findings made during this study. Information in this section is based on written communication from the SFWMD (R. Van Zee, South Florida Water Management District, May 20, 1996). Subsequent changes may have been made.

The Atlantic Ocean boundary condition for the ground-water system is specified as a stage boundary. In NSM version 4.3, the stage boundaries were specified to be the ends (eastern face) of the boundary cells. Because of the staggered nature of the grid (fig. 3), this boundary condition resulted in a discontinuous ground-water boundary at the Atlantic Ocean. The ground-water boundary was made continuous in the NSM 4.4 by specifying the boundary conditions at the northern, eastern, or southern faces of the boundary cells, as appropriate.

Overland-flow velocities (eqs. 31 and 32) in NSM version 4.3 were mistakenly multiplied by the factor $(|z_{i,j,t} - z_{i+1,j,t+1}|)^{1/2}$ for the computation of $u_{i,j,t+1}$, and by the factor $(|z_{i,j,t} - z_{i,j-1,t+1}|)^{1/2}$ for the computation of $v_{i,j,t+1}$, when the computations proceeded from west to east and north to south. Analogous factors were misapplied when the computations proceeded in the east to west and south to north directions. This coding error was corrected in the NSM 4.4.

Sensitivity tests by the SFWMD indicated that a 6-hour time step is more desirable than a 24-hour time step for overland-flow computations. Consequently, a “time-slicing” routine was added to NSM version 4.4. (This capability was included in earlier versions of the model, but not in the version reviewed by the USGS.) The overland-flow system equations are solved at 6-hour intervals in the NSM 4.4, while the ground-water and river-system equations are solved at 24-hour time

intervals. In addition, an alternating-direction numerical scheme was implemented to reduce bias introduced by the manner in which the overland-flow equations are numerically solved. The alternating-direction scheme can only be used when the number of time slices per day is a multiple of 4 (or time steps of 6 hours, 3 hours, 1.5 hours, and so on).

Reducing the computational time interval for the overland-flow system reduces (but does not eliminate) the need to apply the volume limiter described by equation 34. The effects of using different time steps to solve the overland-flow and river systems, which are coupled in a significant manner (fig. 13), are unknown. The river system appears to have a minor effect on the total water balance in the model domain.

Other changes included removing a volume check on the discharge to storage in the rivers and updating overland-flow roughness and evapotranspiration parameters in NSM version 4.4 to be consistent with the corresponding version of the SFWMM. Additional options were added for writing simulation results, and some obsolete code was removed from the model.

Average annual ponding depths simulated with NSM version 4.4 and 1965–90 input data were generally lower than those simulated by using the NSM 4.3. The greatest difference was in the Caloosahatchee River Basin (3.8 ft or less), with smaller changes along the southwest boundary of the ENP (1.3 ft or less). Other changes in ponding depth were less than 1 ft. Hydroperiods in the ENP were changed 20 days or less. Flow patterns simulated with the two versions of the NSM were somewhat the same, with the NSM 4.4 simulations showing more flow toward the Caloosahatchee River and more concentrated flow in the Shark River Slough instead of the relatively uniform flow across the Tamiami Trail simulated with the NSM 4.3

Conclusions

Fundamental (or theoretical) inconsistencies in model formulations should not be ignored, even if the effects of such inconsistencies in model results appear to be insignificant or have not been clearly defined. As a result of this review and ongoing discussions, changes to NSM version 4.3 were made by SFWMD staff during this investigation. Because those changes have already been made, they are not included as part of the conclusions in this section. Conclusions from the

review of the NSM governing equations, numerical scheme, and implementation are summarized as follows:

- The development of automated routines to perform range checking on input data sets and boundary data would help ensure that incorrect values were not included in these data files. As an example of the need for such routines, apparently erroneous input data and initial conditions were found in 1965 input data files. Corrections to these files, if needed, can be made easily.

- The effects of changes in initial conditions remain in the model for more than 1 year. At a minimum, the first 2 years of simulation results should be omitted from the analysis of results. An alternative, and perhaps preferred, scenario for eliminating the effects of initial conditions on simulation results is to apply the model by using 1965–90 mean boundary conditions as the first 2 or more years of input data for the simulation period.

- Simulated mean ponding depth, depth to ground water, and hydroperiod are generally insensitive to changes in the magnitude of the computational time step. This is true when either a 2-mi or a 2/3-mi computational cell size is used. The area of the model domain which was simulated as being dry changed less than 2 percent with changes in the time step from 24 to 0.05 hours.

- The historic water level, ponding depth, depth to ground water, and hydroperiod are unknown. For NSM version 4.3, simulated ponding depths are somewhat dependent on the magnitude of the grid size. Moreover, the magnitude of the standard deviations of the differences between NSM version 4.3 results and results obtained with the 2/3-mi grid is on the order of the maximum ponding depths in much of the model domain. However, simulated mean depth to ground water and hydroperiod both appear to be unaffected by changes in grid size and time step.

- A model is considered to be convergent if a decrease in the size of the time or space step results in no appreciable change in model results. The fact that simulated ponding depths are a function of grid size does not necessarily mean that the model algorithms are incorrect or that an inappropriate numerical scheme has been used to solve the equations. Rather, the size of the spatial finite difference used to discretize the continuous differential equations probably has not been chosen appropriately for the particular problem.

Consequently, the simulations appear to remain a function of the magnitude of the grid size.

- There is no limit on the amount of water that can be removed from the recharge term by evapotranspiration when the water level is below land surface. The effect on simulated results of failing to limit evapotranspiration was not determined.

- There is no limit within the NSM on the amount of water that can be transferred from the river system into the overland-flow system, on seepage from the river to the ground-water system, or on evaporation from the river system. Consequently, the solution of the river-system equations can theoretically yield a result in which mass is not conserved. Because most of the water in the NSM is in the overland-flow system and because the rivers are generally remote from the Everglades, the absence of these limitations likely does not affect simulated water levels and hydroperiods in the Everglades.

- Oscillations of 0.2 ft or less in simulated river stage are present at higher river stages for 1965 conditions. Decoupling the river and overland-flow systems apparently eliminated these oscillations, suggesting that the overland-flow system is the source of the oscillations.

- The Manning coefficient, n , used in the simulation of the overland-flow velocities is determined from information at a single computational node, i,j . Velocities, however, are simulated from information in the i,j node and two adjacent nodes. Consequently, the n -value used to compute the velocities would be more representative of the average roughness along the flow path if a length-weighted coefficient were computed from the roughness in the same nodes as those used in the velocity computation, or the i,j node and the appropriate adjacent nodes. Only velocities in nodes which are at the interface of land-use types would be directly affected by this algorithm change, although the effects of these changes in velocity would propagate throughout the entire model domain.

- The NSM includes an algorithm to maintain numerical stability, by limiting the volume of water that can pass from one cell node in a single computational time step. This prevents reversals in water-surface slope. The volume limiter is a function of the grid size and time step, and is generally applied more frequently with a longer time step. The effect of the volume limiter is to retard flows in the region where the limiter is applied. Tests indicated that the volume limiter was

applied almost 15 million times for 1 year of simulations made with the 2-mi grid and a 30-minute time step. This means that the limiting function was applied to about 37 percent of the computations during the 1-year simulation.

- It is likely that the observed oscillations in river stage are a result of application of the volume limiter in the solution of the overland-flow equations. The flow routine attempts to move water through more than one cell during a single time step, but the volume limiter prevents this and levels the water surface between adjacent cells. Then, during the next time step, little or no flow occurs because of the low water-surface gradient. When additional inflow occurs from rainfall or upstream flow, the water-level gradient again increases, and flow increases until the limiter is applied. Theoretically, water will not be propagated at the correct velocity and computed ponding depths will be in error if inappropriate combinations of time step and cell size are used.

- Boundary water-surface elevations for the overland-flow system are not explicitly set at most of the northern (excluding the lakes) and western boundaries of the grid. Consequently, at these nodes where boundaries are not specified, initial conditions and the previously calculated depths are used as the boundary water-surface elevations. Because there is no information on historic ponding depths at the northern and western boundaries of the model domain, this approach for setting boundary water-surface elevations is probably reasonable. The sensitivity of model results to changes in this assumption regarding ponding depth boundary conditions has not been evaluated. Because these boundaries are far from the Everglades, it is unlikely that this assumed boundary condition significantly affects simulated water levels and hydroperiods in the Everglades.

- The no-flow boundary condition for the ground-water system used at all boundaries other than the tidal boundary does not ensure a no-flow condition at the boundary. The appropriate equations for the ground-water elevations at the boundaries are given in equations 47–50. Results from simulations made with 1965 input data and the correct boundary conditions were not significantly different from results obtained using NSM version 4.3.

SUGGESTIONS FOR APPLICATION OF THE NATURAL SYSTEM MODEL

The Natural System Model can be a very useful tool for estimating pre-drainage hydrologic response in south Florida. The model includes all of the important physical processes needed to simulate a water balance. In general, these hydrologic processes are represented in a reasonable manner by using empirical, semi-empirical, and mechanistic relations. The data sets which have been assembled to represent physical features and hydrologic and meteorological conditions are quite extensive in their scope.

All simulation models, including the NSM, represent abstractions of the physical system. As the NSM was developed, choices were made between model complexity and the extent to which the model would (or needed to) represent the physical system. For example, the two-dimensional laterally averaged equations of continuity and momentum, such as those used in the TRIM model, could have been implemented for the NSM rather than the more simple formulations used. However, the simpler approach was judged to provide adequate information at the scale for which the model operates. But, simpler approaches also generally require the use of more model parameters which must be “tuned” during the calibration process. In addition, the larger the computational cell size, the more physical processes are described by parameters rather than by equations governing the physics of the flow processes. An understanding of the limitations of the NSM, including the governing equations, numerical solution of the equations, and input and boundary data, is required to ensure that the model is applied appropriately and results are interpreted correctly.

The recommendations for modifications to the NSM and suggestions for applications presented in this section result from the conclusions reached from this review of the governing equations, the evaluation of NSM version 4.3, and the results of previous investigations. Other issues identified during this review also are summarized in this section.

Suggested Modifications

A few modifications to NSM version 4.4 are suggested. Most of these modifications are relatively easy to implement and will result in a more rigorous model.

- Develop and use automated routines for checking input and boundary data.
- Modify the river algorithm to ensure that mass is conserved.
- Compute Manning n using a length-weighted approach.
- Develop and use automated routines for checking simulated velocities.
- Correct the ground-water boundary condition so that the no-flow condition is maintained.
- Apply the model by using 1965–90 mean boundary conditions as the first 2 or more years of input data for the simulation period to remove the effects of initial conditions from simulated results.

Documentation of the NSM needs to be compiled and published. Model documentation will provide both model users and decision-makers with the comprehensive information needed to help ensure that the NSM is applied appropriately and that simulation results are interpreted correctly. Documentation should include information on the governing equations, numerical solution of the equations, computational grid, assumptions and limitations of the model, input data, model parameters, options available to the user, sensitivity analysis (the relative sensitivity of model results to changes in each parameter), model output, and “quasi-validations.” Thorough documentation of changes made to the model should continue to be maintained. Most of this information is available now in a variety of forms and locations and could be consolidated into a comprehensive, widely available document.

Appropriate Applications

Results from the limited convergence tests made with the 2-mi grid and a range of time steps (tables 2 and 3) indicate that a 30-minute time step is more appropriate for the NSM simulations than larger time steps. Because the NSM parameters are obtained from the calibrated SFWMM, it may then be necessary to calibrate the SFWMM for a 30-minute step, although the effects of discretization size on SFWMM results were not evaluated. Results from the convergence tests seem to agree with independent conclusions (C. McVoy, Environmental Defense Fund, written commun., 1997) that water levels in pre-drainage south Florida were higher than suggested by NSM version 4.4 simulations. In tests conducted during this study, smaller discretizations resulted in larger simulated

ponding depths and smaller depths to ground water (table 2; figs. 8 and 9).

Results from a number of investigations, including this study, clearly indicate that relatively small, but reasonable, changes in the NSM parameters, algorithms, or assumptions can result in changes in ponding depth and water level of at least 1 ft or more. Changes from version 4.3 to version 4.4 of the NSM resulted in differences in simulated ponding depth of as much as 3.8 ft in remote locations of the model domain. Differences between the NSM 4.3 and the NSM 4.4 simulated ponding depths were 1.3 ft or less in the Everglades. Water-level differences between the NSM 4.3 simulations and results using smaller temporal and spatial discretizations were on the order of 0.7 ft (table 3). McVoy (Environmental Defense Fund, written commun., 1997) observed that long-term average annual high and low water levels simulated with the NSM 4.4 were as much as 1.5 ft different from water levels inferred from historic information. Fennema and others (1994) noted that water levels simulated with NSM version 3.4 for natural areas of modern south Florida were within about 1 ft of measured water levels. Finally, ponding depth is a function of the assumed historic land-surface elevation, as well as simulated water level. Pre-drainage land-surface elevation is assumed to be uniform over 4-mi² areas in the NSM, and is not known with a high degree of certainty.

These results demonstrate some of the uncertainty in the NSM simulated water levels and ponding depths. This uncertainty is associated with input data (primarily topography), model assumptions (for example, rainfall and evapotranspiration distributions), parameters (Manning n and evapotranspiration coefficients), model discretization, and to a lesser extent, other factors. The total uncertainty cannot be quantified. However, as shown, reasonable changes in the NSM can result in simulated water levels which differ by a foot or more. For this reason, it seems appropriate to interpret the NSM simulated water levels and ponding depths with about a plus or minus 1 ft uncertainty.

Hydroperiod is a direct function of simulated water level. Consequently, the uncertainty in simulated water levels also is reflected in hydroperiods. Hydroperiods in the ENP simulated by using NSM version 4.3 and version 4.4 differed by 20 days or less.

There is insufficient information to suggest a reporting level for hydroperiods (for example, to the

nearest 1, 10, or 30 days). However, reporting levels for hydroperiods certainly should be consistent with ecological requirements and understanding. For example, there is no valid reason to report hydroperiods to the nearest day, or even 10 days, if the ecological system is insensitive to long-term changes in hydroperiods of this magnitude. Likewise, hydroperiod is arbitrarily, but reasonably, defined as the number of days when the water level is greater than the land-surface elevation. Yet, the difference in the response of the ecosystem to periods of ponding depths of 0.1 ft compared to periods when the water level is 0.1 ft below the ground surface is not well understood. Finally, a hydroperiod of 30 consecutive days of inundated conditions is different from a hydroperiod of 30 days, which includes periods of inundated and dry conditions, so hydroperiods should be interpreted in the context of frequency and duration of inundation.

There is much evidence to suggest that the NSM should not be used to simulate discharges in pre-drainage south Florida. Moreover, the maintenance of acceptable water levels and hydroperiods, rather than flows, is probably the key to restoration of the Everglades (Van Lent and others, 1993). In general, reasonable simulations of water depth are easier to obtain in all hydraulic simulation models than reasonable simulations of flow. This is true even when sufficient data are available to construct and calibrate the model, which is not the case for the NSM. Although historic data indicate that the NSM simulated flow patterns are reasonable, there has been no “quasi-calibration” of simulated flow volumes because of the absence of reliable historic information on flows.

There is some uncertainty about historic Lake Okeechobee water levels and about the elevation of the southern rim of the lake, but a change of 1 ft in either of these values results in a significant change in simulated flow as far south as the Tamiami Trail (Fennema and others, 1994). NSM results are highly sensitive to changes in evapotranspiration parameters, and changes in evapotranspiration are balanced by changes in flow. For example, a 20-percent change in evapotranspiration in NSM version 3.4 resulted in changes in simulated annual flow of from 60 to 73 percent in Shark River Slough (Fennema and others, 1994).

Unexpectedly high velocities are simulated by the NSM version 4.3. Likewise, unusual simulated velocity patterns exist along the northern and western boundaries of the model. Velocity, along with water

depth, is used to compute flow. Velocities are sensitive to land-surface slope, but historic topographic information remains questionable. Sensitivity tests of the river algorithms also suggest that there are numerical instabilities in the overland-flow algorithm. Frequent application of the volume limiter in the overland-flow routines certainly affects simulated flows in a manner that has not been clearly documented. The Manning n is not known with any degree of certainty, particularly in the areas of the NSM domain which are developed or drained in the SFWMM. But simulated flows, particularly during dry years, are sensitive to the value of the Manning coefficient, although simulated water levels and hydroperiods are fairly insensitive to changes in the Manning coefficient (Fennema and others, 1994).

Tests of the river algorithm indicated that changing the river outflow condition from a weir to the Manning formulation resulted in significant changes in stage and, thus, flow in the river. Both the Manning and the weir formulations appear to be valid. However, the NSM-simulated flows in the rivers have generally been of limited interest.

The NSM is a regional-scale model (Fennema and others, 1994), and results need to be interpreted at a regional scale rather than cell by cell. Vegetation and topography, which vary continuously across the landscape, are assumed to be uniform within each 4-mi² computational cell. This assumption is appropriate for simulating regional flow processes. However, attempts to extract meaningful hydrologic information from a single cell ignores the effects of intracell variations which might include tree islands, secondary flow channels, and topographic variations. There is some uncertainty about the historic vegetation and topographic data which were used to create the NSM grid. Topographic and vegetation data used in the NSM for any one cell may be significantly different from historic conditions, but there is good evidence that the vegetation and topographic data do represent regional variations. This, then, further emphasizes the need to avoid focusing analysis of simulated results on any one computational cell. Finally, restoration efforts are to be for the entire system rather than for isolated areas; the regional perspective provided by the NSM is appropriate for this type of restoration approach.

Simulation results for certain topographic features, which are only 2 to 4 grid cells in width, need to be carefully interpreted. Examples might include Taylor Slough and portions of the Atlantic Coastal

Ridge. If topographic changes actually occur within a cell, the computational cell smooths topographic variations which are abrupt at the boundaries of the features, resulting in simulations that represent an average of conditions adjacent to and within the feature. Moreover, the numerical scheme used to solve the overland-flow equations uses information in the unknown cell and an adjacent cell. Hence, conditions near the eastern and western edges of Taylor Slough, for example, would be solved by using information from within the slough and from cells adjacent to the slough.

Several investigators have cautioned against using NSM results from computational cells near model boundaries. The effects on simulations of the estimated boundary water-level conditions at the northern and western boundaries, the assumed weir-crest elevations in the rivers, and the monthly mean tidal elevations at ocean boundaries do not reflect daily and inter-annual variations. Consequently, a high degree of confidence cannot be placed in simulated hydrologic conditions near model boundaries. Unfortunately, “near” remains subjective, because the spatial extent to which boundary conditions significantly affect simulations in the model interior is not known. However, tests of changes in evapotranspiration parameters indicated that the effects were apparent within about five computational cells of the cell in which the change was made. Hence, at a minimum, simulated results for locations within about 10 mi (five 2-mi cells) of model boundaries should be evaluated cautiously until further information on boundary effects are known. Boundary effects, however, should be of little consequence in the evaluation of hydrologic response of pre-drainage Everglades, because most of the Everglades region is not near a boundary.

Results from the NSM need to be interpreted in connection with other types of information. The work by McVoy (Environmental Defense Fund, written commun., 1997) and the “quasi-validations” are good examples of using NSM results with other available data. Present restoration plans appear to be focused on meeting the NSM or “NSM-like” targets for water level and hydroperiod. However, restoration success likely will be judged on ecological criteria, rather than on the ability of the water-management system to meet certain hydrologic targets. Much stronger linkages between hydrologic conditions and biological response are needed.

Issues for Possible Further Investigation

Some additional issues relating to the NSM and interpretation of simulation results were identified during this review. It may be appropriate to address these issues during future investigations or at the time the model documentation is prepared.

Abtew and others (1993) recommended that optimal interpolation or kriging methods be used to estimate rainfall in ungaged areas of south Florida. Replacing the current NSM algorithm for estimating rainfall in ungaged areas, which is done by assuming that the rainfall in the ungaged cell is equal to rainfall at the nearest gage, with a more rigorous method could lead to changes in simulation results. A more rigorous method would avoid discontinuities in rainfall amounts at adjacent computational cells, and likely would lead to greater model credibility.

Chin and Zhao (1995) concluded that universal kriging provided better estimates of reference-crop evapotranspiration in south Florida than the empirical Penman-Monteith equation. Because the NSM simulation results are so sensitive to evapotranspiration parameters, universal kriging might be investigated as an alternative to the 11 evapotranspiration basins presently used in the NSM.

A number of investigators have cautioned against using NSM results that are near a boundary (Van Lent and others, 1993; Fennema and others, 1994). However, the extent to which boundary conditions affect simulated results in the model domain and near the boundaries has not been quantified. Further investigation may provide insight into the uncertainty associated with simulated results near model boundaries.

REFERENCES

- Abtew, W., Obeysekera, J., and Shih, G., 1993, Spatial analysis for monthly rainfall in south Florida: *Water Resources Bulletin*, v. 29, no. 2, p. 179–188.
- Ames, W.F., 1992, *Numerical methods for partial differential equations* (3d ed.): San Diego, Calif., Academic Press, Inc., p. 126–128.
- Bear, Jacob, 1979, *Hydraulics of groundwater*: New York, McGraw-Hill, p. 111–114.
- Bidlake, W.R., Woodham, W.M., and Lopez, M.A., 1993, *Evapotranspiration from areas of native vegetation in west-central Florida*: U.S. Geological Survey Open-File Report 93–415, 35 p.

- Casulli, V., 1990, Semi-implicit finite-difference methods for the two-dimensional shallow water equations: *Journal of Computational Physics*, v. 86, p. 56–74.
- Cheng, R.T., and Casulli, V., 1992, Tidal residual, intertidal mudflat (TRIM) model using semi-implicit Eulerian-Lagrangian method: U.S. Geological Survey Open-File Report 92–62.
- Chin, D.A., and Zhao, S., 1995, Evaluation of evaporation-pan networks: *Journal of Irrigation and Drainage Engineering*, American Society of Civil Engineers, v. 121, no. 5, p. 338–346.
- Conte, S.D., 1980, *Elementary numerical analysis, an algorithmic approach* (3d ed.): New York, McGraw-Hill, p. 74–80.
- Fennema, R.J., 1992, *Natural System Model, An evaluation of version 3.4*: Homestead, Fla., Report to the National Park Service, Everglades National Park.
- Fennema, R.J., Neidrauer, C.J., Johnson, R.A., MacVicar, T.K., and Perkins, W.A., 1994, A computer model to simulate natural Everglades hydrology, *in* Davis, S.M., and Ogden, J.C., eds., *Everglades, The ecosystem and its restoration*: Delray Beach, Fla., St. Lucie Press, p. 249–289.
- Guardo, M., and Tomasello, R.S., 1995, Hydrodynamic simulations of a constructed wetland in south Florida: *Water Resources Bulletin*, v. 31, no. 4, p. 687–701.
- Lapidus, L., and Pinder, G.F., 1982, *Numerical solution of partial differential equations in science and engineering*: New York, John Wiley and Sons.
- Linsley, R.K., Jr., Kohler, M.A., and Paulhus, J.L.H., 1975, *Hydrology for engineers* (2d ed.): New York, McGraw-Hill, p. 294–300.
- Loucks, D.P., and Stedinger, J.R., 1994, Sensitivity and uncertainty analysis in hydrologic simulation modeling of the South Florida Water Management District: Ithaca, N.Y., Report of the Workshop on Reduction of Uncertainties in Regional Hydrologic Simulation Models (SFWMM and NSM), 62 p.
- MacVicar, T.K., Van Lent, T., and Castro, A., 1984, *South Florida water management model documentation report*: West Palm Beach, South Florida Water Management District, Technical Publication 84–3.
- Perkins, W.A., and MacVicar, T.K., 1991, A computer model to simulate natural south Florida hydrology: West Palm Beach, South Florida Water Management District, draft report.
- Roache, P.J., 1982, *Computational fluid dynamics*: Albuquerque, N.M., Hermosa Publishers, 446 p.
- Thompson, D.B., 1992, Numerical methods 101—convergence of numerical models, *in* Jennings, M.E., and Bhowmik, N.G., eds., *Hydraulic engineering, saving a threatened resource—in search of solutions*: New York, American Society of Civil Engineers, p. 398–403.
- Trimble, P.J., 1995, An evaluation of the certainty of system performance measures generated by the South Florida Water Management Model: Boca Raton, Fla., Department of Civil Engineering, Florida Atlantic University, unpublished M.S. thesis, 549 p.
- Van Lent, T., 1995, *Using the Natural System Model as a basis for water management in Shark Slough, Everglades National Park*: Homestead, Fla., Report to the Everglades National Park, 68 p.
- Van Lent, T., Johnson, R., and Fennema, R., 1993, *Water management in Taylor Slough and effects on Florida Bay*: Homestead, Fla., South Florida Research Center, Everglades National Park, National Park Service, 79 p. + app.

APPENDIX—List of Variables

a_m	Surface area of the river associated with the m river node.
A_{gw}	Surface area for the ground-water system.
A_o	Surface area for overland flow.
A_r	Total surface area of the river system.
b_w	Weir width.
c	A constant to maintain proper unit conversion in Manning's equation.
d	Depth from land surface to the shallow root zone.
D	Depth from land surface to the deep root zone.
e_m	Potential evaporation.
E_o	Evapotranspiration from the overland-flow system.
E_r	Evaporation from the river system.
E_{max_m}	Maximum evapotranspiration coefficient.
f_m	Fall in the water surface at the m river node.
F_r	Total water-surface elevation change over an entire river system.
g	Acceleration of gravity
h or h_m	Elevation of the ground-water surface.
H or $H_{m,t}$	Overland-flow ponding depth.
i	East-west location of the computed node in the grid.
I_o	Infiltration to the ground-water system.
j	North-south location of the computed node in the grid.
k	Evapotranspiration coefficient that varies as a function of time and land-use type.
k_w	Weir coefficient.
K_m	Seepage coefficient.
L_m	Distance to the river node measured from the downstream end of the river system.
L_r	Total length of the river system.
M	Total number of river nodes in a river system.
m	Location of river node in a river.
n or n_m	Manning's coefficient of roughness.
$O_{i,j}$	Open-water ponding depth.
P_o	Precipitation on the overland-flow system.
P_r	Precipitation on the river system.
q_{t+1}	River system inflow specified at the $t+1$ time step.
Q_f	Flow between the river system and the overland system.
Q_{gw}	Flow from the ground-water system to the overland system.
Q_o	Flow due to overland flow between cells.
Q_r	Flow into and out of the ends of the river system.
R_{gw}	Total ground-water recharge.
R_r	Flow between the river system and the ground-water system or recharge.
S	Storage coefficient in ground-water equation.

S_s	Soil storage coefficient.
t	Time.
t^*	An intermediate time step used in overland-flow calculations.
T_{xx}	Aquifer transmissivities in x -direction.
T_{yy}	Aquifer transmissivities in y -direction.
u	Overland-flow velocity in the x -direction.
v	Overland-flow velocity in the y -direction.
V_{gw}	Water volume associated with the ground-water system.
V_o	Water volume associated with the overland-flow system.
V_r	Water volume associated with the river systems.
V_T	Total water volume in the NSM model.
w_{el}	Weir crest elevation.
Y or Y_r	River stage or water-surface elevation for the river system.
z	Water-surface elevation.
Z_m	Land-surface elevation.
Z_{tide}	Water elevation due to tide.
∂	Partial derivative operator.
Γ_m	Flow depth, which is a function of flow conditions.
Δt	Time-step size.
Δx	Grid spacing in the x -direction.
Δy	Grid spacing in the y -direction.
Ω	Coriolis parameter.
ρ	Water density.
$\tau_{b,x}, \tau_{b,y}$	Bed shear stresses acting in the x - and y -directions, respectively.
$\tau_{s,x}, \tau_{s,y}$	Surface shear (wind) stresses acting in the x - and y -directions, respectively.
$\tau_{xx}, \tau_{xy}, \tau_{yx}, \tau_{yy}$	Shear stresses caused by turbulence.
α	The flow angle with respect to the x -axis.
β	The flow angle with respect to the y -axis.
δ_m	Detention depth.
κ	Hydraulic conductivity.
ζ	Aquifer depth measured from a common datum.